

# An analysis of the accuracy of the linear sampling method for an acoustic inverse obstacle scattering problem

Nguyen Trung Thành\* and Mourad Sini

Johann Radon Institute for Computational and Applied Mathematics (RICAM),  
Austrian Academy of Sciences

Email addresses: trung-thanh.nguyen@oeaw.ac.at, mourad.sini@oeaw.ac.at

\*Corresponding author.

## Abstract

We investigate the accuracy of the linear sampling method for a two-dimensional acoustic inverse obstacle scattering problem with Dirichlet boundary condition using asymptotic analysis of the so-called indicator function around the boundary of the obstacle. An asymptotic expansion of the limit, as the noise level and the regularization parameter tend to zero, of the indicator function is obtained. The theoretical results show the dependence of the blowup rate of this limit on geometrical properties of the obstacle. This partly (up to the above limit) explains the dependence of the accuracy of the linear sampling method on the obstacle's geometry. Some numerical results are given to verify the theoretical results.

**Keywords:** Linear sampling method, inverse obstacle scattering problem, Dirichlet boundary condition, asymptotic expansion, numerics.

## 1 Introduction and motivation

Inverse obstacle scattering problems have been considered by the mathematical and engineering communities for a long time. Their main objective is to reconstruct the shape of an obstacle from measurements of scattered fields of, e.g., acoustic, electromagnetic or elastic fields.

In this paper, we consider the scattering of time-harmonic acoustic plane waves by a two-dimensional sound-soft obstacle  $D \in \mathbb{R}^2$ . We assume that the boundary of  $D$  is smooth enough (the precise smoothness required will be given in Section 3). The scattered field  $u^s$  of an incident wave  $u^i$  can be represented as the solution to the following two-dimensional Dirichlet boundary value problem [6]

$$\Delta u^s(x) + \kappa^2 u^s(x) = 0, \quad x \in \mathbb{R}^2 \setminus \bar{D}, \quad (1)$$

$$u^s(x) = -u^i(x), \quad x \in \partial D, \quad (2)$$

$$\lim_{r \rightarrow \infty} \sqrt{r} \left( \frac{\partial u^s(x)}{\partial r} - i\kappa u^s(x) \right) = 0, \quad r = |x|, \quad (3)$$

where  $\kappa$  is the wave number. In the above system, the equation (3) is called the Sommerfeld radiation condition, which guarantees the unique solvability of the problem (1)–(2).

The well-posedness of the problem (1)–(3) is well-known (see, e.g., [6, 13]). To state the inverse problem, we first recall that the asymptotic behavior of the scattered field  $u^s$  at infinity can be represented by

$$u^s(x) = \frac{e^{i\kappa r}}{\sqrt{r}} u^\infty(\hat{x}) + O(r^{-3/2}), \quad r \rightarrow \infty, \quad (4)$$

where  $\hat{x} := x/r$  and  $u^\infty$  is an analytic function on the unit circle  $\mathbb{S}^1 := \{x \in \mathbb{R}^2 : |x| = 1\}$  referred to as the *far field pattern* of the scattered field  $u^s$ . In the case of an incident plane wave, i.e.,  $u^i(x) = e^{i\kappa x \cdot d}$ , with  $d \in \mathbb{S}^1$  being the direction of propagation, we denote the far field pattern by  $u^\infty(\hat{x}, d)$  to emphasize its dependence on the incident direction.

With the above notation, we can state the inverse obstacle scattering problem using far field measurements as follows: *Given the far field pattern  $u^\infty(\hat{x}, d)$ ,  $\hat{x} \in \mathbb{S}^1$ , for one or several incident directions  $d \in \mathbb{S}^1$ , find the domain  $D$ .*

Regarding the uniqueness and stability issues of the above problem, we refer the reader to [6, 9].

In this paper, we make use of the measured data for *all* incident directions  $d \in \mathbb{S}^1$  and consider the linear sampling method for solving the above inverse problem. It is a non-iterative method which was firstly introduced by Colton and Kirsch in 1996 [5]. So far, this method has been investigated by many researchers (see, e.g. [4, 10] and the references therein). In the linear sampling method, an indicator function of one spatial variable is defined based on the solution of the so-called *far field equation*. The main idea of this method relies on the property that the indicator function is bounded in the interior of the obstacle  $D$  and explodes at the boundary of  $D$  as well as in the external region (see more details in a short summary in Section 2). Then, the boundary of the obstacle is determined as the location at which the indicator function starts to blow up.

Although numerical results indicate a good performance of the linear sampling method, there are still some open questions that have not been fully resolved yet (see Section 2). One of them, which is the main focus of this paper, is on the accuracy of the method. This accuracy relates closely to the blowup rate of the indicator function around the boundary of the obstacle. If the indicator function blows up uniformly around the boundary, the method will certainly provide accurate estimates. On the contrary, if the blowup rate is different from point to point, it may be difficult to obtain an accurate estimate of the obstacle. The reconstruction accuracy may be different for different obstacles or different parts of an obstacle (for example, convex versus concave parts).

In this paper, we investigate the effect of geometrical properties of the obstacle on the accuracy of the linear sampling method. More precisely, we provide an asymptotic expansion of the limit, as the noise level and the regularization parameter tend to zero, of the indicator function when its variable tends to the boundary of the obstacle from inside. The asymptotic expansion shows that the blowup rate of this limit near the boundary of the obstacle depends on the curvature of the boundary of the obstacle (see Remark 3.4 for more detailed discussions about the true indicator function). This partly (up to the limit as the noise level and the regularization parameter tend to zero) explains why obstacles with uniform

curvature can be detected with more accuracy than obstacles with non-uniform curvature. This approach has been studied by one of the authors and his coworkers for the probe method [11, 12]. The extension of the approach to the linear sampling method is based on: (i) the property that the Herglotz wavefunctions, with densities given by the approximate solutions of the far field equation using Tikhonov regularization, converge to the solution of an interior Dirichlet boundary value problem with point sources as boundary conditions, as justified in [1, 2]; and (ii) the asymptotic expansion of the solution of this interior problem near the boundary of the obstacle.

The rest of the paper is organized as follows. In the next section, we recall with some details the basis of the linear sampling method and its convergence property. The detail analysis of the asymptotic expansion mentioned above is given in Section 3. In Section 4, we illustrate the analysis using some numerical examples. In this section we also give some numerical results comparing the accuracy of the linear sampling method for multipoles of different orders which are used in obtaining the aforementioned asymptotic expansion. Some concluding remarks are given in Section 5.

## 2 The linear sampling method

In the first part of this section, we briefly summarize the basis of the linear sampling method. For more details, we refer to [4, 5]. In the second part, we recall the results by Arens [1] and Arens and Lechleiter [2] on the convergence of the linear sampling method, see also [10]. After that, we discuss the accuracy issue of the linear sampling method which is the main focus of this paper.

### 2.1 The basis of the linear sampling method

Given the far field pattern  $u^\infty(\hat{x}, d)$  (see (4)) of the scattered field of the forward problem (1)–(3) with the incident plane wave  $u^i(x) = e^{i\kappa x \cdot d}$  for  $d \in \mathbb{S}^1$ , we define the so-called *far field operator*  $F : L^2(\mathbb{S}^1) \rightarrow L^2(\mathbb{S}^1)$  corresponding to (1)–(3) as follows

$$(Fg)(\hat{x}) = \int_{\mathbb{S}^1} u^\infty(\hat{x}, d)g(d)ds(d) \text{ for } g \in L^2(\mathbb{S}^1), \hat{x} \in \mathbb{S}^1. \quad (5)$$

The fundamental properties of the far field operator needed to state the linear sampling method are summarized in the following lemma, see [4, 5, 10].

**Lemma 2.1.** *If  $\kappa^2$  is not a Dirichlet eigenvalue of the negative Laplacian  $-\Delta$  in  $D$ , then the far field operator  $F$  is linear, bounded, injective, compact and has a dense range in  $L^2(\mathbb{S}^1)$ .*

The linear sampling method is based on the analysis of the solution to the far field equation

$$(Fg_z)(\hat{x}) = \Phi^\infty(\hat{x}, z), \hat{x} \in \mathbb{S}^1, z \in \mathbb{R}^2, \quad (6)$$

where  $\Phi^\infty(\hat{x}, z)$  is the far field pattern of the fundamental solution  $\Phi(x, z)$  of the Helmholtz equation given by

$$\Phi(x, z) = \frac{i}{4} H_0^{(1)}(\kappa|x - z|), \quad (7)$$

with  $H_0^{(1)}$  being the Hankel function of the first kind of order zero. Using the asymptotic expansion of the Hankel function at infinity and (4), we obtain the explicit formula for the far field pattern of the fundamental solution

$$\Phi^\infty(\hat{x}, z) = \frac{e^{i\pi/4}}{\sqrt{8\pi\kappa}} e^{-i\kappa\hat{x}\cdot z}.$$

The following theorem is the fundamental result of the linear sampling method, see [4].

**Theorem 2.2.** *Suppose that  $\kappa^2$  is not a Dirichlet eigenvalue of the negative Laplacian  $-\Delta$  in  $D$ . Then we have*

1. *If  $z \in D$ , then for every  $\epsilon > 0$ , there exists a solution  $g_z \in L^2(\mathbb{S}^1)$  of the inequality*

$$\|Fg_z - \Phi^\infty(\cdot, z)\|_{L^2(\mathbb{S}^1)} < \epsilon \quad (8)$$

*such that  $\lim_{z \rightarrow \partial D} \|g_z\|_{L^2(\mathbb{S}^1)} = +\infty$  and  $\lim_{z \rightarrow \partial D} \|v_{g_z}\|_{H^1(D)} = +\infty$ .*

2. *If  $z \notin D$ , then for every  $\delta > 0$  and  $\epsilon > 0$ , there exists a solution  $g_z \in L^2(\mathbb{S}^1)$  of the inequality*

$$\|Fg_z - \Phi^\infty(\cdot, z)\|_{L^2(\mathbb{S}^1)} < \epsilon + \delta \quad (9)$$

*such that  $\lim_{\delta \rightarrow 0^+} \|g_z\|_{L^2(\mathbb{S}^1)} = +\infty$  and  $\lim_{\delta \rightarrow 0^+} \|v_{g_z}\|_{H^1(D)} = +\infty$ ,*

where  $v_{g_z}$  is the Herglotz wavefunction with density  $g_z$  defined by

$$v_{g_z}(x) = \int_{\mathbb{S}^1} e^{i\kappa x \cdot d} g_z(d) ds(d), \text{ for all } x \in \mathbb{R}^2. \quad (10)$$

We note that the  $H^1(D)$ -norm of  $v_{g_z}$  cannot be calculated because  $D$  is unknown. Therefore, in the next subsection on the convergence of the linear sampling method, it is replaced by  $|v_{g_z}(z)|$ , which can be directly calculated using (10) given the solution  $g_z$ .

In practice, the far field operator cannot be given exactly since the measured far field pattern always contains noise. Therefore, the operator  $F$  is replaced by  $F^\delta$  such that  $\|F^\delta - F\| < \delta$ , where  $\delta$  is the noise level and  $\|\cdot\|$  is the operator norm. Moreover, the two inequalities (8) and (9) are usually replaced by a regularized version of the far field equation. For example, using the Tikhonov regularization technique, we arrive at the following equation

$$[\alpha I + (F^\delta)^* F^\delta] g_{z,\alpha}^\delta = (F^\delta)^* \Phi^\infty(\cdot, z), \quad (11)$$

where  $I$  is the identity operator in  $L^2(\mathbb{S}^1)$ ,  $(F^\delta)^*$  is the adjoint operator of  $F^\delta$  and  $\alpha$  is the regularization parameter. In this equation we write  $g_{z,\alpha}^\delta$  to emphasize the dependence of the solution on the noise level and the regularization parameter. This equation is equivalent to the minimization problem [4]

$$g_{z,\alpha}^\delta = \operatorname{argmin} \|F^\delta g_{z,\alpha}^\delta - \Phi^\infty(\cdot, z)\|_{L^2(\mathbb{S}^1)}^2 + \alpha \|g_{z,\alpha}^\delta\|_{L^2(\mathbb{S}^1)}^2. \quad (12)$$

Note that the regularization parameter  $\alpha$  depends on  $\delta$  and  $z$  and must be chosen in an appropriate way in order to guarantee the convergence of the solution of (12) to the solution of the far field equation (6).

One of the optimal choices of this parameter is based on Morozov's discrepancy principle. That is,  $\alpha$  is chosen by solving the implicit equation

$$\|F^\delta g_{z,\alpha}^\delta - \Phi^\infty(\cdot, z)\|_{L^2(\mathbb{S}^1)}^2 - \delta^2 \|g_{z,\alpha}^\delta\|_{L^2(\mathbb{S}^1)}^2 = 0. \quad (13)$$

Given the solution of the regularized far field equation, we can define an indicator function  $I(z)$  with the expected property that its values in the interior and exterior of  $D$  are considerably different. For example, we can choose  $I(z) := \|g_{z,\alpha}^\delta\|$  or  $I(z) := \|g_{z,\alpha}^\delta\|^{-1}$ .

Based on Theorem 2.2 and the above analysis, the common implementation of the linear sampling algorithm with Tikhonov regularization can be briefly described as follows

1. Choose a set of sampling points in a region covering the expected obstacle.
2. For each sampling point  $z$ , find a regularization parameter  $\alpha$  and an approximate solution of the regularized far field equation (11) such that (13) is satisfied.
3. Calculate the indicator function  $I(z)$ .
4. Use some cut-off value  $C$  to determine an approximation  $D_a$  of  $D$  by asserting that  $z \in D_a$  iff  $I(z) < C$  (or  $I(z) > C$ , depending the behavior of the chosen indicator function).

Note that apart from the cut-off procedure for choosing the approximation of the shape, there are also other post-processing methods available in the literature, see e.g. [3].

## 2.2 Convergence of the linear sampling method

In many published works, the above algorithm provides good reconstructions of the shapes, even though we cannot always guarantee the solution of the regularized equation (11) converges to a function having the properties mentioned in Theorem 2.2. This issue was addressed in [1, 2, 8] for the case of Dirichlet boundary condition and Tikhonov regularization method. In [1, 2], the authors used the well-justified factorization method (see [10]) to prove the aforementioned assertion. In addition, they proved the convergence of the Herglotz wavefunction  $v_{g_{z,\alpha}^\delta}$ , with the solution to the regularized equation (11) being its density, to  $-\Phi(\cdot, z)$  in  $H^{1/2}(\partial D)$  as the noise level  $\delta$  tends to zero for  $z \in D$  if the regularization parameter is chosen such that  $\alpha \rightarrow 0$  and  $\delta/\alpha^{3/2} \rightarrow 0$  as  $\delta$  tends to zero. This implies that the Herglotz wavefunction explodes near  $\partial D$ . For  $z \notin D$ , the authors also showed that  $|v_{g_{z,\alpha}^\delta}(z)|$  (i.e., in the absence of noise) tends to infinity (see also [10]). Hence, from [1, 2] we have the following theorem which proves the convergence of the linear sampling method, at least for the noise-free data.

**Theorem 2.3.** *Let  $g_{z,\alpha}^\delta(\cdot)$  be the solution of the regularized equation (11) with the regularization parameter chosen such that  $\alpha \rightarrow 0$  and  $\delta/\alpha^{3/2} \rightarrow 0$  as  $\delta$  tends to zero. Then*

1. *If  $z \in D$ , we have  $|v_{g_{z,\alpha}^\delta}(z)| < +\infty$  and  $\lim_{z \rightarrow \partial D} \lim_{\delta \rightarrow 0} |v_{g_{z,\alpha}^\delta}(z)| = +\infty$ .*
2. *If  $z \notin D$ , we have  $\lim_{\alpha \rightarrow 0} |v_{g_{z,\alpha}^\delta}(z)| = +\infty$  (i.e., for the noise-free data).*

The result for  $z \notin D$  for noisy data is still an open question.

### 2.3 The accuracy issue of the linear sampling method

Another issue, which is related to the numerical accuracy of the linear sampling method, is that the cut-off constant  $C$  in the linear sampling algorithm is usually fixed for all sampling points. However, the blowup rate of the indicator function  $I(z)$  may depend on physical and geometrical properties of the boundary of the obstacle. Hence, the accuracy of the reconstruction may depend on the properties of the boundary  $\partial D$ . To our best knowledge, this issue has not been analyzed in the literature regarding the linear sampling method. This issue is the main focus of this paper. More precisely, we give an explicit blowup rate of  $\lim_{\alpha \rightarrow 0} |v_{g_{z,\alpha}}(z)|$  (or  $\lim_{\delta \rightarrow 0} |v_{g_{z,\alpha}^\delta}(z)|$  for  $\alpha(\delta)$  and  $\delta/\alpha^{3/2}$  tend to zero as  $\delta \rightarrow 0$ ) when  $z$  tends to  $\partial D$  from inside. This is presented in the next section.

## 3 Main results: Asymptotic expansion

In this section, we are mainly interested in the Herglotz wavefunction  $v_{g_{z,\alpha}^\delta}$  and hence consider  $|v_{g_{z,\alpha}^\delta}(z)|$  as the indicator function. Our main purpose in this section is to derive the blowup rate of  $\lim_{\delta \rightarrow 0} |v_{g_{z,\alpha}^\delta}(z)|$  when the sampling point  $z$  tends to the boundary of the obstacle from inside, i.e., in the first case of Theorem 2.3, since this limit should explode in the exterior domain  $\mathbb{R}^2 \setminus D$ .

As shown later, the aforementioned blowup rate is low (of logarithmic order) if the far field of the fundamental solution is used as the right hand side of the regularized far field equation (11). Therefore, the involvement of the curvature does not clearly show up in this case. In order to better demonstrate this involvement, we use not only the far field of the fundamental solution (*monopole*) but also its first derivatives (*dipoles*) and second derivatives (*tripoles*) as the right hand side of (11). Therefore in this section, we consider the following general regularized far field equation

$$(\alpha I + (F^\delta)^* F^\delta) g_{z,\alpha}^\delta = (F^\delta)^* \psi^\infty(\cdot, z), \quad (14)$$

where  $\psi^\infty(\cdot, z)$  is the far field pattern of the function  $\psi(x, z)$  which is one of the following cases

$$\begin{aligned} 1) \psi(x, z) &= \Phi(x, z), & 2.1) \psi(x, z) &= \frac{\partial \Phi(x, z)}{\partial z_1}, & 2.2) \psi(x, z) &= \frac{\partial \Phi(x, z)}{\partial z_2} \\ 3.1) \psi(x, z) &= \frac{\partial^2 \Phi(x, z)}{\partial z_1^2}, & 3.2) \psi(x, z) &= \frac{\partial^2 \Phi(x, z)}{\partial z_1 \partial z_2}, & 3.3) \psi(x, z) &= \frac{\partial^2 \Phi(x, z)}{\partial z_2^2}. \end{aligned} \quad (15)$$

It is easy to verify from (7) that  $\frac{\partial^2 \Phi(x, z)}{\partial z_1^2} = -\frac{\partial^2 \Phi(x, z)}{\partial z_2^2}$ . Hence, in the following, we will omit Case 3.3.

The main idea of our approach in analyzing the behavior of the indicator function near the boundary of the obstacle is as follows. We first show the convergence of  $v_{g_{z,\alpha}^\delta}(z)$  to  $\varphi(z, z)$  (as  $\delta$  tends to zero), where  $\varphi(x, z)$  is the solution to the interior Dirichlet boundary value problem

$$\begin{cases} \Delta \varphi(x, z) + \kappa^2 \varphi(x, z) = 0, & x \in D, \\ \varphi(x, z) = -\psi(x, z), & x \in \partial D, \end{cases} \quad (16)$$

and then investigate the asymptotic behavior of  $\varphi(z, z)$  as  $z$  tends to the boundary of  $D$ . Note that the function  $\psi(\cdot, z)|_{\partial D}$  given in (15) explodes as  $z$  tends to  $\partial D$ . For the clarity of the two above steps, we state them in the following separate subsections.

### 3.1 Convergence of $v_{g_{z,\alpha}^\delta}(z)$ to $\varphi(z, z)$

Using the same arguments as in [1], Theorem 3.3 and Corollary 3.4, and [2], we can justify the following result.

**Theorem 3.1.** *Consider an arbitrary but fixed sampling point  $z \in D$  and let  $v_{g_{z,\alpha}^\delta}$  be the Herglotz wavefunction with density  $g_{z,\alpha}^\delta$  being the solution to the regularized far field equation (14). Moreover, the regularization parameter is chosen so that both  $\alpha$  and  $\delta/\alpha^{3/2}$  tend to zero as  $\delta \rightarrow 0$ . Then we have*

$$\lim_{\delta \rightarrow 0} \left\| v_{g_{z,\alpha}^\delta}|_{\partial D} + \psi(\cdot, z)|_{\partial D} \right\|_{H^{1/2}(\partial D)} = 0$$

and hence,

$$\lim_{\delta \rightarrow 0} |v_{g_{z,\alpha}^\delta}(z) - \varphi(z, z)| = 0, \quad (17)$$

where  $\varphi(x, z)$  is the solution of the interior Dirichlet boundary value problem (16).

We note that as stated in [2], the hypothesis of Theorem 3.1 is valid when the regularization parameter  $\alpha$  is chosen using the generalized Morozov discrepancy principle.

### 3.2 Asymptotic expansion of $\varphi(z, z)$ as $z$ tends to $\partial D$

We consider the asymptotic behavior of  $\varphi(z, z)$  as  $z \in D$  tends to an arbitrary but fixed point  $a \in \partial D$ . For this purpose, we need to assume that  $\partial D \in C^{2,1}$ , i.e., there exists a rigid coordinate transformation under which  $a = 0$  and there exists a positive value  $r$  such that  $\bar{D} \cap B(0, r) = \{\bar{x} \in \mathbb{R}^2 : \bar{x}_2 > f_a(\bar{x}_1)\}$ , where  $\bar{D}$  is the considered domain in the new coordinate system and the function  $f_a \in C^{2,1}(-r, r)$  satisfies  $f_a(0) = 0$ ,  $f'_a(0) = 0$ . The main result of this section is stated in the following theorem.

**Theorem 3.2 (Main result).** *Suppose that the boundary of the obstacle  $D$  is of class  $C^{2,1}$ . Let  $a$  be an arbitrary point on  $\partial D$  with out-ward unit normal vector  $\nu(a)$ . We denote by  $C(a, \theta)$  the cone with vertex  $a$ , axis  $-\nu(a)$  and an arbitrary but fixed angle  $\theta \in [0, \frac{\pi}{2})$ . Then, the solution  $\varphi(x, z)$  of the interior problem (16), with the boundary condition  $\psi(x, z)$  given by (15), has the following asymptotic expansion as  $z \in D \cap C(a, \theta)$  tends to  $a$ :*

1) For  $\psi = \Phi(x, z)$  :

$$\varphi(z, z) = \frac{1}{2\pi} \ln |(z - a) \cdot \nu(a)| + O(1). \quad (18)$$

2) For  $\psi = \frac{\partial}{\partial z_j} \Phi(x, z)$ ,  $j \in \{1, 2\}$  :

$$\varphi(z, z) = -\frac{\nu_j(a)}{4\pi |(z - a) \cdot \nu(a)|} + O(1). \quad (19)$$

3.1) For  $\psi = \frac{\partial^2}{\partial z_1^2} \Phi(x, z)$  :

$$\begin{aligned} \varphi(z, z) &= \frac{\nu_2^2(a) - \nu_1^2(a)}{8\pi |(z - a) \cdot \nu(a)|^2} - \frac{[\nu_2^2(a) - \nu_1^2(a)]f''_a(0)}{16\pi |(z - a) \cdot \nu(a)|} \\ &+ \frac{\nu_1(a)\nu_2(a)f''_a(0)}{4\pi |(z - a) \cdot \nu(a)|} \tan \theta_{za} + O(\ln(|(z - a) \cdot \nu(a)|)). \end{aligned} \quad (20)$$

3.2) For  $\psi = \frac{\partial^2}{\partial z_1 \partial z_2} \Phi(x, z)$ :

$$\begin{aligned} \varphi(z, z) = & -\frac{\nu_1(a)\nu_2(a)}{4\pi|(z-a)\cdot\nu(a)|^2} + \frac{\nu_1(a)\nu_2(a)f_a''(0)}{8\pi|(z-a)\cdot\nu(a)|} \\ & + \frac{[\nu_2^2(a) - \nu_1^2(a)]f_a''(0)}{8\pi|(z-a)\cdot\nu(a)|} \tan \theta_{za} + O(\ln(|(z-a)\cdot\nu(a)|)). \end{aligned} \quad (21)$$

Here  $\theta_{za}$  is the angle between the vector  $z-a$  and  $\nu(a)$  which is defined to be positive if the rotation from  $z-a$  to  $\nu(a)$  is clockwise and negative if the rotation is anticlockwise.

Before proving this theorem, let us first give some remarks on its use in explaining the accuracy of the linear sampling method.

*Remark 3.3.* In the case of tripoles (20) and (21), the curvature of the boundary  $\partial D$  is involved in the first order singularity of  $\varphi(z, z)$ . However, the blowup rate of  $\varphi(z, z)$  near a point  $a$  depends on the normal  $\nu(a)$  of  $\partial D$  at  $a$  (this is also true for the dipoles). In order to avoid the effect of the location on the blowup rate, we consider the combined function

$$\varphi(z, z) = [\varphi_{3.1}^2(z, z) + \varphi_{3.2}^2(z, z)]^{1/2},$$

where  $\varphi_{3.1}^2(z, z)$  and  $\varphi_{3.2}^2(z, z)$  are given by (20)–(21), respectively. Note that the subscripts are used just to clarify the considered cases. Moreover, if we approach  $a$  in the normal direction, i.e.,  $\theta_{za} = 0$ , it follows from (20) and (21) that

$$\varphi(z, z) = \left[ \frac{1}{64\pi^2|z-a|^4} - \frac{f_a''(0)}{64\pi^2|z-a|^3} + O\left(\frac{1}{|z-a|^2}\right) \right]^{1/2}, \text{ for } z \text{ near } a. \quad (22)$$

From this equation we can see that if the curvature is uniform, the level curves of  $\varphi(z, z)$  should provide similar shapes as  $\partial D$  (up to the effect of the lower order terms) when they are "close enough" to the boundary. On the contrary, if the curvature is non-uniform, the blowup rate will vary from point to point, especially when the curvature changes its sign.

In the cases of the monopole and dipoles, i.e., in (18) and (19), the curvature does not appear in the singular terms of the asymptotic expansion of  $\varphi(z, z)$ . However, the curvature should be involved in the bounded terms. This does not contradict the case of tripoles because the blowup rate of  $\varphi(z, z)$  in the first two cases is slower than the last one. Numerical results in Section 4 show that the effect of the curvature on the accuracy of the linear sampling method is observable in all cases.

*Remark 3.4.* We note that Theorem 3.2 only provides the asymptotic expansions of  $\lim_{\delta \rightarrow 0} v_{g_z, \alpha}^\delta(z)$  as  $z \rightarrow \partial D$ . Therefore, this theorem can only partly explain (up to the limit as the noise level and the regularization parameter tend to zero) the blowup rate of the indicator function of the linear sampling method. Concerning the original indicator function  $v_{g_z, \alpha}$ , in [2], the authors gave an estimate of the following form for noise-free data (monopole)

$$2\pi\|g_z\|_{L^2(\mathbb{S}^2)}^2 - M \leq |v_{g_z, \alpha}(z)| \leq 4\pi\|g_z\|_{L^2(\mathbb{S}^2)}^2, \text{ for } \alpha \leq \alpha_0(z),$$

where  $g_z$  is the solution to the equation  $(F^*F)^{1/4}g_z = \Phi^\infty(\cdot, z)$  in the Factorization method. A kind of estimates should also be true for multipoles. Taking into account the result of Hähner [7] on the blowup rate of  $g_z$ , we can obtain lower and upper bounds of the indicator function  $|v_{g_z, \alpha}(z)|$  of the form (for the tripoles)

$$\frac{C_l}{\text{dist}(z, \partial D)^2} \leq |v_{g_z, \alpha}(z)| \leq \frac{C_u}{\text{dist}(z, \partial D)^2}, \text{ for } \alpha \leq \alpha_0(z),$$

with  $0 < C_l < C_u$  and  $\text{dist}(z, \partial D)$  being the distance from  $z$  to  $\partial D$ . However, it is not possible to show the involvement of the curvature of the obstacle in the indicator function in this kind of lower and upper estimates since the curvature only appears in lower singular terms. Moreover, this is also a pointwise estimate because the regularization parameter  $\alpha$  depends on the sampling point  $z$ . Indeed, if this estimate is valid uniformly, then the regularized indicator function  $|v_{g_z, \alpha}(z)|$ , for a small enough  $\alpha$  independent of  $z$ , will tend to infinity at  $\partial D$ . This is not possible! Therefore, Theorem 3.2 seems to be the best possible result (to our best knowledge) that we can obtain about the asymptotic behavior of the indicator function.

*Remark 3.5.* Since in this paper we consider the Dirichlet boundary condition, physical properties of the obstacle are not involved in the indicator function. However, when the obstacle satisfies, for instance, the impedance boundary condition, we can derive a similar blowup rate of  $\varphi(z, z)$  as in Theorem 3.2 to show the dependence of the indicator function on the geometrical as well as physical properties of the obstacle. Moreover, in design problems, we can choose the physical parameters in such a way that the singular term in the expansion containing the curvature and the physical parameters is either very small (so the blowup rate becomes more uniform, this is for better detection) or large (so the blowup rate becomes less uniform, this is for better hiding). This is known as *coating* procedure. This problem is under investigation (see [11, 12] for the coating using the probe method).

We now turn to the proof of Theorem 3.2. The following lemma on asymptotic expansions of the fundamental solution of the Helmholtz equation and its derivatives plays a central role in the proof. These results can be obtained using asymptotic expansions of Bessel functions (see also [6]).

**Lemma 3.6.** *Denote by  $\Phi(x, z)$  the fundamental solution of the Helmholtz equation in  $\mathbb{R}^2$ . Then we have the following asymptotic expansions as  $|x - z|$  tends to zero:*

$$1) \Phi(x, z) = \frac{1}{2\pi} \ln \frac{1}{|x - z|} + \frac{i}{4} - \frac{1}{2\pi} \ln \frac{\kappa}{2} - \frac{C_E}{2\pi} + O(|x - z|^2 \ln |x - z|), \quad (23)$$

$$2) \frac{\partial \Phi(x, z)}{\partial x_j} = -\frac{1}{2\pi} \frac{x_j - z_j}{|x - z|^2} + O(|x - z| \ln |x - z|), \quad j = 1, 2, \quad (24)$$

$$3) \frac{\partial^2 \Phi(x, z)}{\partial x_1^2} = \frac{1}{2\pi} \frac{(x_1 - z_1)^2 - (x_2 - z_2)^2}{|x - z|^4} + O(\ln |x - z|) = -\frac{\partial^2 \Phi(x, z)}{\partial x_2^2}, \quad (25)$$

$$4) \frac{\partial^2 \Phi(x, z)}{\partial x_1 \partial x_2} = \frac{1}{\pi} \frac{(x_1 - z_1)(x_2 - z_2)}{|x - z|^4} + O(\ln |x - z|), \quad (26)$$

with  $C_E$  being the Euler's constant ( $C_E \approx 0.5772$ ).

We note that since the fundamental solution  $\Phi(x, z)$  is symmetric, the derivatives of  $\Phi(x, z)$  with respect to  $z$  have similar asymptotic expansions as (23)–(26), just taking care with the signs.

**Proof of Theorem 3.2.** For each fixed point  $a \in \partial D$ , with out-ward unit normal vector  $\nu(a)$ , we consider the coordinate transformation  $\bar{x} = R(x - a)$ , where  $R$  is the rotation matrix defined by

$$R = \begin{pmatrix} -\nu_2(a) & \nu_1(a) \\ -\nu_1(a) & -\nu_2(a) \end{pmatrix}.$$

Under this coordinate transformation, the point  $a$  becomes the origin and its normal vector  $\nu(a)$  becomes

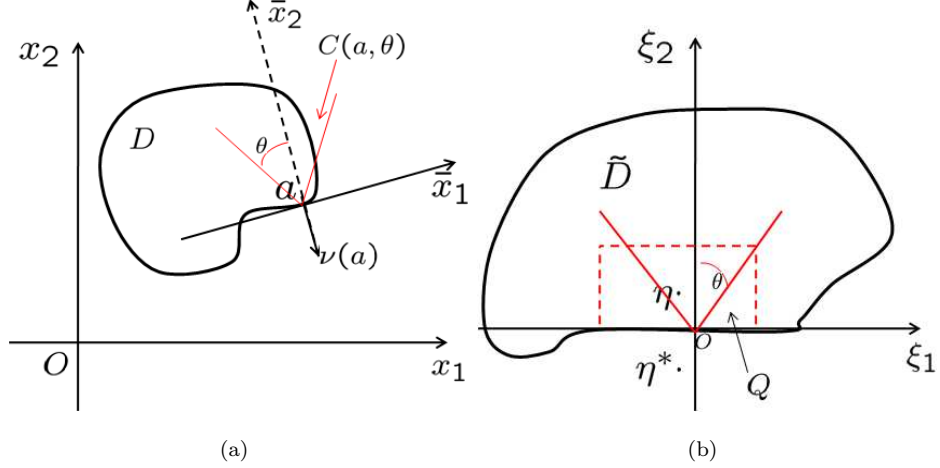


Figure 1: Coordinate transformations: (a) from  $x$  to  $\bar{x}$ ; (b) in  $\xi$ -coordinate system.

$(0, -1)^T$  in the  $\bar{x}$ -coordinate system, i.e.,  $R\nu(a) = (0, -1)^T$  (see Figure 1(a)). We denote by  $\bar{D}$  the obstacle in the new coordinate system. We also denote by  $\bar{\varphi}(\bar{x}, \bar{z}) = \varphi(x, z)$  and  $\bar{\Phi}(\bar{x}, \bar{z}) = \Phi(x, z)$ . Note that since the distance function is invariant under rotation and translation, we have  $\bar{\Phi}(\bar{x}, \bar{z}) = \Phi(\bar{x}, \bar{z})$ . However, in this new coordinate system, we have

$$\frac{\partial}{\partial z_i} \Phi(x, z) = (R_i^c)^T \nabla_{\bar{z}} \Phi(\bar{x}, \bar{z}), \quad (27)$$

$$\frac{\partial^2}{\partial z_i \partial z_j} \Phi(x, z) = \left( A_{ij}^1 \frac{\partial^2}{\partial \bar{z}_1^2} + A_{ij}^2 \frac{\partial^2}{\partial \bar{z}_1 \partial \bar{z}_2} + A_{ij}^3 \frac{\partial^2}{\partial \bar{z}_2^2} \right) \Phi(\bar{x}, \bar{z}), \quad (28)$$

with  $(R_i^c)^T$  being the transpose of the  $i$ th-column of  $R$  and  $A_{ij}^1 = R_{1i}R_{1j}$ ,  $A_{ij}^2 = R_{1i}R_{2j} + R_{1j}R_{2i}$  and  $A_{ij}^3 = R_{2i}R_{2j}$ . Therefore, it follows from (16) that the function  $\bar{\varphi}(\bar{x}, \bar{z})$  satisfies the problem

$$\begin{cases} \Delta_{\bar{x}} \bar{\varphi}(\bar{x}, \bar{z}) + \kappa^2 \bar{\varphi}(\bar{x}, \bar{z}) = 0, & \bar{x} \in \bar{D}, \\ \bar{\varphi}(\bar{x}, \bar{z}) = -\bar{\psi}(\bar{x}, \bar{z}), & \bar{x} \in \partial \bar{D}, \end{cases} \quad (29)$$

where  $\bar{\psi}(\bar{x}, \bar{z}) = \psi(x, z)$ . In the following, we only consider the asymptotic expansion of  $\bar{\varphi}(\bar{z}, \bar{z})$  as  $\bar{D} \ni \bar{z} \rightarrow 0$  (equivalently,  $z \rightarrow a$ ). From (15), (27) and (28) we have the following cases

$$1) \bar{\psi}(\bar{x}, \bar{z}) = \Phi(\bar{x}, \bar{z}) \quad (30)$$

$$2.1) \bar{\psi}(\bar{x}, \bar{z}) = - \left[ \nu_2(a) \frac{\partial}{\partial \bar{z}_1} + \nu_1(a) \frac{\partial}{\partial \bar{z}_2} \right] \Phi(\bar{x}, \bar{z}) \quad (31)$$

$$2.2) \bar{\psi}(\bar{x}, \bar{z}) = \left[ \nu_1(a) \frac{\partial}{\partial \bar{z}_1} - \nu_2(a) \frac{\partial}{\partial \bar{z}_2} \right] \Phi(\bar{x}, \bar{z}) \quad (32)$$

$$3.1) \bar{\psi}(\bar{x}, \bar{z}) = \left\{ [\nu_2^2(a) - \nu_1^2(a)] \frac{\partial^2}{\partial \bar{z}_1^2} + 2\nu_1(a)\nu_2(a) \frac{\partial^2}{\partial \bar{z}_1 \partial \bar{z}_2} \right\} \Phi(\bar{x}, \bar{z}) \quad (33)$$

$$3.2) \bar{\psi}(\bar{x}, \bar{z}) = \left\{ -2\nu_1(a)\nu_2(a) \frac{\partial^2}{\partial \bar{z}_1^2} + [\nu_2^2(a) - \nu_1^2(a)] \frac{\partial^2}{\partial \bar{z}_1 \partial \bar{z}_2} \right\} \Phi(\bar{x}, \bar{z}) \quad (34)$$

We note that for the cases (31)–(34), we only have to derive the asymptotic expansion of  $\bar{\varphi}$  when  $\bar{\psi}$  is given by

$$2.1) \bar{\psi}(\bar{x}, \bar{z}) = \frac{\partial \Phi(\bar{x}, \bar{z})}{\partial \bar{z}_1}, \quad 2.2) \bar{\psi}(\bar{x}, \bar{z}) = \frac{\partial \Phi(\bar{x}, \bar{z})}{\partial \bar{z}_2}, \quad (35)$$

$$3.1) \bar{\psi}(\bar{x}, \bar{z}) = \frac{\partial^2 \Phi(\bar{x}, \bar{z})}{\partial \bar{z}_1^2}, \quad 3.2) \bar{\psi}(\bar{x}, \bar{z}) = \frac{\partial^2 \Phi(\bar{x}, \bar{z})}{\partial \bar{z}_1 \partial \bar{z}_2}, \quad (36)$$

and then use the superposition of the solutions of (29) and (31)–(34) to arrive at the equations (19)–(21).

For studying the asymptotic expansion of  $\bar{\varphi}(\bar{z}, \bar{z})$ , we first extend  $f_a$  to the whole  $\bar{x}_1$ -axis with constant values far from the origin. For the sake of simplicity, we still denote this extended function by  $f_a$ . Let us consider the coordinate transformation  $\xi = \Theta(\bar{x})$  defined by

$$\begin{cases} \xi_1 = \bar{x}_1, \\ \xi_2 = \bar{x}_2 - f_a(\bar{x}_1). \end{cases}$$

Under this transformation, the domain  $\bar{D}$  is transformed into the domain  $\tilde{D}$  as shown in Figure 1(b) with a part of its boundary near the origin lies on the  $\xi_1$ -axis. Using the notation  $\tilde{\varphi}(\xi, \eta) = \bar{\varphi}(\bar{x}, \bar{z})$ , with  $\xi = \Theta(\bar{x})$  and  $\eta = \Theta(\bar{z})$ , we arrive at the following problem in the  $\xi$ -coordinate system

$$\begin{cases} \nabla \cdot [M \nabla \tilde{\varphi}(\xi, \eta)] + \kappa^2 \tilde{\varphi}(\xi, \eta) = 0, & \xi \in \tilde{D}, \\ \tilde{\varphi}(\xi, \eta) = -\bar{\psi}(\Theta^{-1}(\xi), \Theta^{-1}(\eta)), & \xi \in \partial \tilde{D}, \end{cases} \quad (37)$$

where  $M = JJ^T$ , with  $J$  being the Jacobian of the coordinate transformation, i.e.

$$J = \begin{pmatrix} \frac{\partial \xi_1}{\partial \bar{x}_1} & \frac{\partial \xi_1}{\partial \bar{x}_2} \\ \frac{\partial \xi_2}{\partial \bar{x}_1} & \frac{\partial \xi_2}{\partial \bar{x}_2} \end{pmatrix} = \begin{pmatrix} 1 & 0 \\ -f'_a(\xi_1) & 1 \end{pmatrix}. \quad (38)$$

From this equation we have

$$M = \begin{pmatrix} 1 & -f'_a(\xi_1) \\ -f'_a(\xi_1) & 1 + (f'_a(\xi_1))^2 \end{pmatrix}. \quad (39)$$

It is easily seen that  $M$  is positive definite, hence (37) is well-defined. We now compare the function  $\tilde{\varphi}(\xi, \eta)$  with the solution  $\omega^+(\xi, \eta)$  of the following Dirichlet boundary value problem in the upper half space

$$\begin{cases} \Delta \omega^+(\xi, \eta) + \kappa^2 \omega^+(\xi, \eta) = 0, & \xi \in \mathbb{R}_+^2, \\ \omega^+(\xi, \eta) = -\bar{\psi}(\xi, \eta), & \xi \in \partial \mathbb{R}_+^2, \\ \omega^+(\xi, \eta) \text{ satisfies the Sommerfeld radiation condition.} \end{cases} \quad (40)$$

Denote by  $\tilde{R}(\xi, \eta) = \tilde{\varphi}(\xi, \eta) - \omega^+(\xi, \eta)$ , then it follows from (37) and (40) that  $\tilde{R}(\xi, \eta)$  satisfies the problem

$$\begin{cases} \nabla \cdot [M\nabla\tilde{R}(\xi, \eta)] + \kappa^2\tilde{R}(\xi, \eta) = \nabla \cdot [(I - M)\nabla\omega^+(\xi, \eta)], & \xi \in \tilde{D} \cap \mathbb{R}_+^2, \\ \tilde{R}(\xi, \eta) = -[\tilde{\psi}(\Theta^{-1}(\xi), \Theta^{-1}(\eta)) - \tilde{\psi}(\xi, \eta)], & \xi \in \partial\tilde{D} \cap \partial\mathbb{R}_+^2. \end{cases} \quad (41)$$

We will show in the following that the highest singularities of  $\varphi(x, z)$  (or equivalently,  $\tilde{\varphi}(\xi, \eta)$ ) shown in the theorem come from those of  $\omega^+(\xi, \eta)$  while  $\tilde{R}(\xi, \eta)$  contains the lower singularities. However, these lower singularities might involve the geometrical properties of  $\partial D$ . In order to investigate the properties of  $\tilde{R}(\xi, \eta)$ , we make use of the Green's function of the half space

$$\begin{cases} \nabla \cdot [M\nabla G(\xi, \eta)] + \kappa^2 G(\xi, \eta) = -\delta(\xi - \eta), & \xi \in \mathbb{R}_+^2, \\ G(\xi, \eta) = 0, & \xi \in \partial\mathbb{R}_+^2, \\ G \text{ satisfies the Sommerfeld radiation condition.} \end{cases} \quad (42)$$

We now consider two fixed values  $r_1, r_2 > 0$  such that the rectangle  $Q = \{(\xi_1, \xi_2) : -r_1 + \eta_1 \leq \xi_1 \leq r_1 + \eta_1, 0 \leq \xi_2 \leq r_2\}$  lies totally in  $\tilde{D}$  (see Figure 1(b)). We denote by  $S = \partial Q \cap \partial\mathbb{R}_+^2$  and  $S^c = \partial Q \setminus S$ . We recall that  $\eta \in Q \cap C(0, \theta)$ . Multiplying both sides of the first equation of (41) by  $G(\xi, \eta)$  and both sides of the first equation of (42) by  $\tilde{R}(\xi, \eta)$ , taking the difference and integrating it over  $Q$ , we obtain

$$\begin{aligned} & \int_Q \left[ \nabla \cdot (M\nabla\tilde{R}(\xi, \eta))G(\xi, \eta) - \nabla \cdot (M\nabla G(\xi, \eta))\tilde{R}(\xi, \eta) \right] d\xi \\ &= \int_Q \nabla \cdot [(I - M)\nabla\omega^+(\xi, \eta)]G(\xi, \eta) d\xi + \tilde{R}(\eta, \eta). \end{aligned}$$

Integrating by parts the first and the second integrals, we have

$$\begin{aligned} & \int_{\partial Q} M\nabla\tilde{R}(\xi, \eta) \cdot \nu G(\xi, \eta) ds(\xi) - \int_Q M\nabla\tilde{R}(\xi, \eta) \cdot \nabla G(\xi, \eta) d\xi \\ & - \int_{\partial Q} M\nabla G(\xi, \eta) \cdot \nu\tilde{R}(\xi, \eta) ds(\xi) + \int_Q M\nabla G(\xi, \eta) \cdot \nabla\tilde{R}(\xi, \eta) d\xi \\ &= \int_{\partial Q} (I - M)\nabla\omega^+(\xi, \eta) \cdot \nu G(\xi, \eta) ds(\xi) - \int_Q (I - M)\nabla\omega^+(\xi, \eta) \cdot \nabla G(\xi, \eta) d\xi + \tilde{R}(\eta, \eta), \end{aligned}$$

where  $\nu$  is the out-ward unit normal to  $\partial Q$ . Since  $M$  is symmetric (see (39)), the second and the fourth terms on the left hand side cancel each other. Taking into account the boundary conditions in (41) and (42), we obtain

$$\begin{aligned} \tilde{R}(\eta, \eta) &= \int_{S^c} M\nabla\tilde{R}(\xi, \eta) \cdot \nu G(\xi, \eta) ds(\xi) - \int_{S^c} M\nabla G(\xi, \eta) \cdot \nu\tilde{R}(\xi, \eta) ds(\xi) \\ & - \int_S M\nabla G(\xi, \eta) \cdot \nu\tilde{R}(\xi, \eta) ds(\xi) - \int_{S^c} (I - M)\nabla\omega^+(\xi, \eta) \cdot \nu G(\xi, \eta) ds(\xi) \\ & + \int_Q (I - M)\nabla\omega^+(\xi, \eta) \cdot \nabla G(\xi, \eta) d\xi. \end{aligned}$$

As will be shown in the following, the integrands are only singular at  $\xi = \eta$  and  $\xi = \eta^*$ , where  $\eta^*$  is the image point of  $\eta$  over the  $\xi_1$ -axis, i.e.  $\eta^* = (\eta_1, -\eta_2)$  (see Figure 1(b)). Therefore, when  $\eta \rightarrow 0$ , say,  $|\eta_1| < r_1/2, \eta_2 < r_2/2$ , the integrals on  $S^c$  are bounded. Then, we can write the above equation in the short form

$$\tilde{R}(\eta, \eta) = I_1 - I_2 + O(1), \quad (43)$$

where

$$I_1 = \int_Q (I - M) \nabla \omega^+(\xi, \eta) \cdot \nabla G(\xi, \eta) d\xi \text{ and } I_2 = \int_S M \nabla G(\xi, \eta) \cdot \nu \tilde{R}(\xi, \eta) ds(\xi). \quad (44)$$

The asymptotic behaviors of  $I_1$  and  $I_2$  are given in the following lemmas.

**Lemma 3.7.** *The integral  $I_1$  is bounded for  $\bar{\psi}(\bar{x}, \bar{z}) = \Phi(\bar{x}, \bar{z})$  or  $\bar{\psi}(\bar{x}, \bar{z}) = \frac{\partial}{\partial \bar{z}_j} \Phi(\bar{x}, \bar{z})$ ,  $j \in \{1, 2\}$ , and for  $\bar{\psi}(\bar{x}, \bar{z}) = \frac{\partial^2}{\partial \bar{z}_j \partial \bar{z}_l} \Phi(\bar{x}, \bar{z})$ ,  $j, l \in \{1, 2\}$ , we have*

$$I_1 = O(\ln \eta_2) \text{ as } \tilde{D} \cap C(0, \theta) \ni \eta \rightarrow 0.$$

**Lemma 3.8.** *The integral  $I_2$  is bounded for  $\bar{\psi}(\bar{x}, \bar{z}) = \Phi(\bar{x}, \bar{z})$  or  $\bar{\psi}(\bar{x}, \bar{z}) = \frac{\partial}{\partial \bar{z}_j} \Phi(\bar{x}, \bar{z})$ ,  $j \in \{1, 2\}$ . For  $\bar{\psi}(\bar{x}, \bar{z}) = \frac{\partial^2}{\partial \bar{z}_1^2} \Phi(\bar{x}, \bar{z})$  we have*

$$I_2 = \frac{f''_a(0)}{16\pi\eta_2} + O(\ln \eta_2), \quad (45)$$

while for  $\bar{\psi}(\bar{x}, \bar{z}) = \frac{\partial^2}{\partial \bar{z}_1 \partial \bar{z}_2} \Phi(\bar{x}, \bar{z})$  we have

$$I_2 = -\frac{f''_a(0)\eta_1}{8\pi\eta_2^2} + O(\ln \eta_2) \quad (46)$$

as  $\tilde{D} \cap C(0, \theta) \ni \eta \rightarrow 0$ .

Since the proofs of these two lemmas are quite technical, we postpone them until the Appendix to make the proof of Theorem 3.2 easier to follow. Using these lemmas, we write  $\tilde{\varphi}(\eta, \eta)$  as

$$\tilde{\varphi}(\eta, \eta) = \omega^+(\eta, \eta) + \tilde{R}(\eta, \eta) = \omega^+(\eta, \eta) + I_1 - I_2 + O(1).$$

The behavior of the function  $\omega^+(\xi, \eta)$  depends on the singularity of the function  $\bar{\psi}$  given in (30), (35) or (36). More precisely, using Lemma 3.6, we have

- 1) For  $\bar{\psi}(\bar{x}, \bar{z}) = \Phi(\bar{x}, \bar{z})$ , then  $\omega^+(\xi, \eta) = -\Phi(\xi, \eta^*)$ . Hence,  $\omega^+(\eta, \eta) = \frac{1}{2\pi} \ln \eta_2 + O(1)$ . From this and Lemmas 3.7 and 3.8 we arrive at

$$\tilde{\varphi}(\eta, \eta) = \frac{1}{2\pi} \ln \eta_2 + O(1). \quad (47)$$

- 2.1) For  $\bar{\psi}(\bar{x}, \bar{z}) = \frac{\partial}{\partial \bar{z}_1} \Phi(\bar{x}, \bar{z})$ , we have

$$\omega^+(\xi, \eta) = -\frac{\partial}{\partial \eta_1} \Phi(\xi, \eta^*) = -\frac{\xi_1 - \eta_1}{2\pi|\xi - \eta^*|^2} + O(1),$$

then  $\omega^+(\eta, \eta) = O(1)$ . Consequently,

$$\tilde{\varphi}(\eta, \eta) = O(1). \quad (48)$$

2.2) Similarly, for  $\bar{\psi}(\bar{x}, \bar{z}) = \frac{\partial}{\partial \bar{z}_2} \Phi(\bar{x}, \bar{z})$ , we obtain

$$\omega^+(\xi, \eta) = -\frac{\partial}{\partial \eta_2} \Phi(\xi, \eta^*) = \frac{\xi_2 + \eta_2}{2\pi|\xi - \eta^*|^2} + O(1).$$

In this case, we have  $\omega^+(\eta, \eta) = \frac{1}{4\pi\eta_2} + O(1)$ . Therefore,

$$\tilde{\varphi}(\eta, \eta) = \frac{1}{4\pi\eta_2} + O(1). \quad (49)$$

3.1) For  $\bar{\psi}(\bar{x}, \bar{z}) = \frac{\partial^2}{\partial \bar{z}_1^2} \Phi(\bar{x}, \bar{z})$ , we have

$$\omega^+(\xi, \eta) = -\frac{\partial^2}{\partial \eta_1^2} \Phi(\xi, \eta^*) = -\frac{(\xi_1 - \eta_1)^2 - (\xi_2 + \eta_2)^2}{2\pi|\xi - \eta^*|^4} + O(\ln|\xi - \eta^*|),$$

then  $\omega^+(\eta, \eta) = \frac{1}{8\pi\eta_2^2} + O(\ln \eta_2)$ . Hence,

$$\tilde{\varphi}(\eta, \eta) = \frac{1}{8\pi\eta_2^2} - \frac{f_a''(0)}{16\pi\eta_2} + O(\ln \eta_2). \quad (50)$$

3.2) Similarly, for  $\bar{\psi}(\bar{x}, \bar{z}) = \frac{\partial^2}{\partial \bar{z}_1 \partial \bar{z}_2} \Phi(\bar{x}, \bar{z})$ , we have

$$\omega^+(\xi, \eta) = -\frac{\partial^2}{\partial \eta_1 \partial \eta_2} \Phi(\xi, \eta^*) = \frac{(\xi_1 - \eta_1)(\xi_2 + \eta_2)}{2\pi|\xi - \eta^*|^4} + O(\ln|\xi - \eta^*|),$$

In this case we have  $\omega^+(\eta, \eta) = O(\ln \eta_2)$ . Therefore,

$$\tilde{\varphi}(\eta, \eta) = \frac{f_a''(0)\eta_1}{8\pi\eta_2^2} + O(\ln \eta_2). \quad (51)$$

We note that  $\frac{\eta_1}{\eta_2} = \tan \theta_{za}$  and  $\eta_2$  is of the same order as  $|(z - a) \cdot \nu(a)|$ . Then, Theorem 3.2 now follows from the equations (30)–(34), (47)–(51) and the superposition of the solutions of (29). The proof is complete.  $\square$

## 4 Numerical verification and analysis

In this section, we illustrate the theoretical results presented in Theorem 3.2, i.e., the influence of the curvature of the obstacle's boundary on the indicator function, using some numerical examples. We first note that the far field patterns of the derivatives of the fundamental solution are given by

$$\begin{aligned} \left( \frac{\partial \Phi(\cdot, z)}{\partial z_j} \right)^\infty(\hat{x}) &= -\frac{i\kappa e^{i\pi/4} \hat{x}_j}{\sqrt{8\pi\kappa}} e^{-i\kappa \hat{x} \cdot z}, j \in \{1, 2\}, \\ \left( \frac{\partial^2 \Phi(\cdot, z)}{\partial z_j \partial z_l} \right)^\infty(\hat{x}) &= -\frac{\kappa^2 e^{i\pi/4} \hat{x}_j \hat{x}_l}{\sqrt{8\pi\kappa}} e^{-i\kappa \hat{x} \cdot z}, j, l \in \{1, 2\}. \end{aligned} \quad (52)$$

In this paper, the measured far field pattern  $u^\infty(\cdot, d)$  is simulated as the solution of the forward problem (1)–(3) which is solved by the integral equation method (see, e.g. [6], Section 3.5). In the next examples, the wave number is fixed at  $\kappa = 1$ . The number of incident directions is chosen to be 64. They are

uniformly distributed on the unit circle. The observation directions are the same as the incident ones. The sampling area is chosen to be the square  $[-3, 3]^2$  with the sampling grid of 0.03 in each direction.

Theorem 3.2 shows that the blowup rate of (the limit of) the indicator function depends on the order of the multipoles used in the far field equation. To numerically confirm this result, we consider as the obstacle the circle  $\{|x| \leq 1.5\}$  and plot the values of the indicator functions  $\|g_{z,\alpha}^\delta\|$  and  $|v_{g_{z,\alpha}^\delta}(z)|$  on the horizontal axis in Figure 2. In this example, the noise level of the far field pattern is set to be 0.01%.

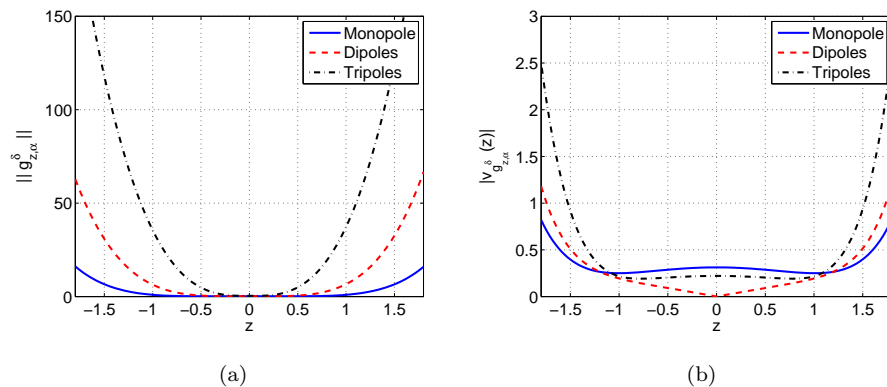


Figure 2: The indicator functions for a circle using the monopole, dipoles and tripoles: (a)  $\|g_{z,\alpha}^\delta\|$ ; (b)  $|v_{g_{z,\alpha}^\delta}(z)|$ . The boundary points are at  $\pm 1.5$ .

The figure shows that the higher the order of the multipole, the higher the values of the indicator functions near the boundary of the obstacle (at  $\pm 1.5$  on the horizontal axis). However, the values of the numerical indicator functions, especially near the boundary of the obstacle, are smaller than the theoretical prediction, which should tend to infinity. In our opinion, this is mostly due to the discretization and regularization of the far field equation (6). Hence, care should be taken in choosing a level curve as an approximation of the obstacle's boundary.

Let us now analyze the effect of the obstacle's geometry on the accuracy of the linear sampling method. Theorem 3.2 predicts that the blowup rate of (the limit of) the indicator function depends on the curvature of the obstacle's boundary, which is represented by the value  $f_a''(0)$ ,  $a \in \partial D$ , (for the monopole and the dipoles, see Remark 3.3). That means, the accuracy of the linear sampling method may be different from point to point if the curvature of the boundary is not uniform. To show this numerically, we consider some kite-shaped obstacles which are represented by the general equation

$$\begin{cases} x_1(t) = \cos t + c(\cos 2t - 1), \\ x_2(t) = \sin t, \end{cases} \quad t \in [0, 2\pi], \quad (53)$$

where  $c$  is a positive parameter which relates to the curvature of the obstacle. In the following, the measurement noise is set to be 3%. As the first example, we consider the kite with  $c = 0.65$  (see Figure 4). Since the numerical solution to the regularized far field equation (14) is large in the exterior

of the obstacle, we use the following normalized indicator functions for better visualization

$$\mathbb{I}^1(z) := (\|g_{z,\alpha}^\delta\| + 1)^{-1}, \quad \mathbb{I}^2(z) := [|v_{g_{z,\alpha}^\delta}(z)| + 1]^{-1}. \quad (54)$$

The behaviors of the normalized indicator functions  $\mathbb{I}^1$  and  $\mathbb{I}^2$  for the kite using the monopole ( $\psi(x, z) = \Phi(x, z)$ ) are depicted in Figure 3.

As discussed in Section 2, the boundary of the obstacle is determined using some cut-off procedure. In this paper, we only analyze level curves of the indicator function  $\mathbb{I}^2(z)$ . They are defined as the set of all sampling points satisfying

$$m + (n - 1) \frac{M - m}{N} \leq \mathbb{I}^2(z) < m + n \frac{M - m}{N},$$

for each  $n = 1, 2, \dots, N$ , where  $m = \min_z \mathbb{I}^2(z)$  and  $M = \max_z \mathbb{I}^2(z)$  and  $N$  is a positive integer determining the number of subintervals that the interval  $[m, M]$  is divided into. In this example, the interval  $[m, M]$  is divided into 100 subintervals, i.e.,  $N = 100$ .

In Figure 4 we plot some level curves of  $\mathbb{I}^2(z)$  for the monopole. This figure shows clearly that the accuracy of the reconstruction depends on the choice of the level curve. However, even when the level curve is suitably chosen, the accuracy may still be different from different parts of the boundary. Indeed, in Figure 4(a), the level curve approximates well the boundary at the corners of the kite (with high curvature) while in the other part, the estimate is less accurate, especially in the concave part of the kite (with negative curvature). In Figure 4(b), the accuracy is worse at the corners but better in the other convex parts. Similar behaviors are shown in Figures 4(c) and 4(d).

The results for the dipoles and tripoles depicted in Figures 5 and 6 also show similar behaviors, i.e. the reconstruction accuracy is different on different parts of the boundary, especially between the convex and concave parts. We can see clearly that if we want to have an accurate reconstruction of the convex part, then we will lose the accuracy on the concave part (Figures 4(c), 5(a) and 6(a)) and vice versa (Figures 4(d), 5(b) and 6(b)).

In order to show the influence of the curvature of the obstacle's boundary on the accuracy, we consider another kite with the constant  $c$  in (53) being set to be 0.1. In this case, the obstacle is convex with more uniform curvature (see Figure 7).

As we can see from Figure 7, the level curves follow the shape of the obstacle much better than the first kite, i.e., the blowup rate of the numerical indicator function is more uniform around the boundary. Of course, we still can see the difference in the reconstruction of different parts with different values of the curvature (compare the top and the bottom with the left and the right sides). We note that for a circle (with the uniform curvature), the reconstruction is really accurate everywhere (with an appropriate level curve).

When the boundary becomes less uniform, the reconstruction becomes worse as shown in Figure 8 for a kite with  $c = 1$ , (in this case,  $f_a''(0)$ ,  $a \in \partial D$ , varies more quickly than the last two cases).

The above numerical results confirm the dependence of the accuracy of the linear sampling method on the curvature of the obstacle's boundary, which is in agreement with the theoretical results presented

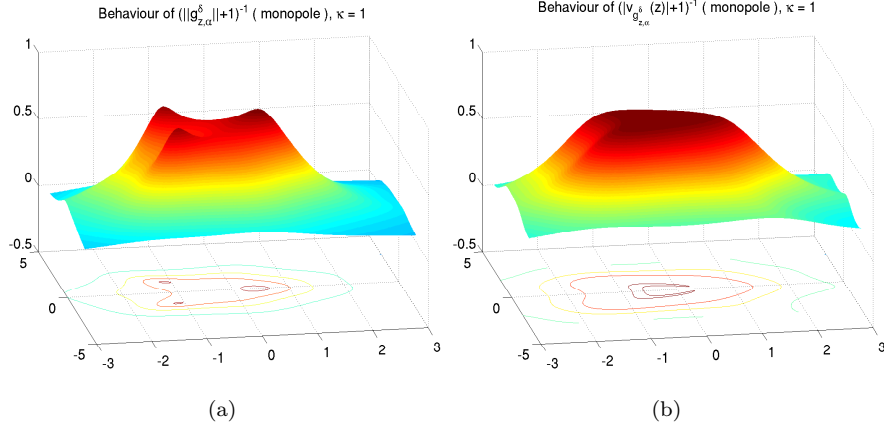


Figure 3: Behaviors of the normalized numerical indicator functions for the kite with  $c = 0.65$  (using the monopole): (a)  $\mathbb{I}^1(z) = (\|g_{z,\alpha}^\delta\| + 1)^{-1}$ ; (b)  $\mathbb{I}^2(z) = [|v_{g_{z,\alpha}^\delta}(z)| + 1]^{-1}$ .

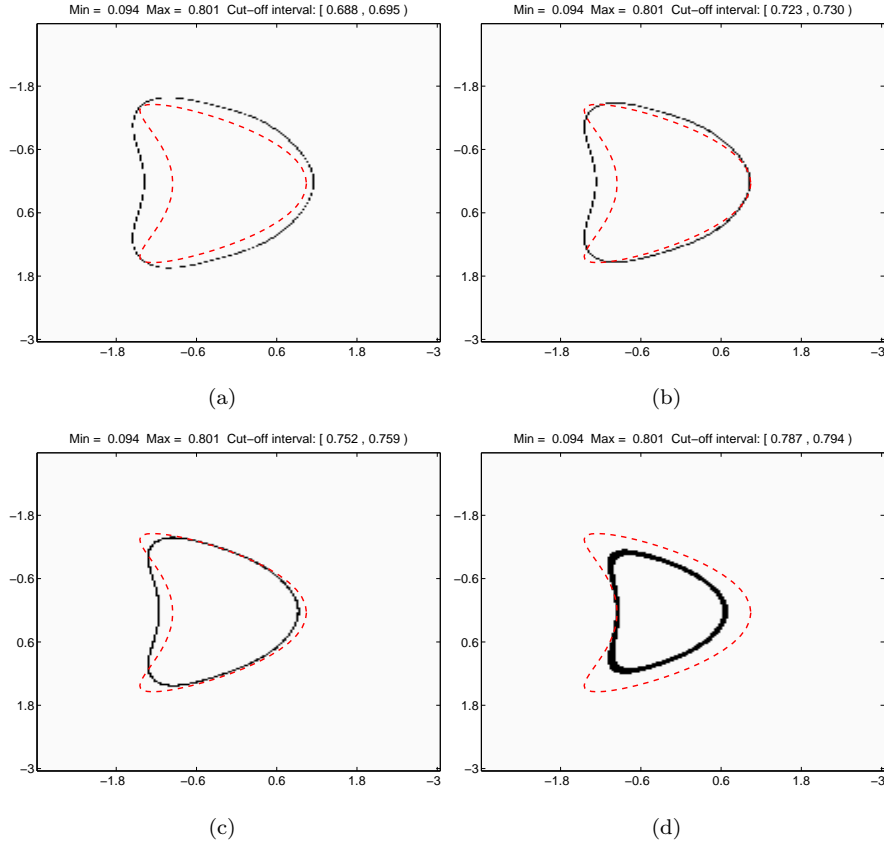


Figure 4: Level curves of  $\mathbb{I}^2(z)$  for the kite with  $c = 0.65$  and  $N = 100$  (using the monopole): (a)  $n = 85$ ; (b)  $n = 90$ ; (c)  $n = 94$ ; (d)  $n = 99$ . The dash curve represents the exact shape.

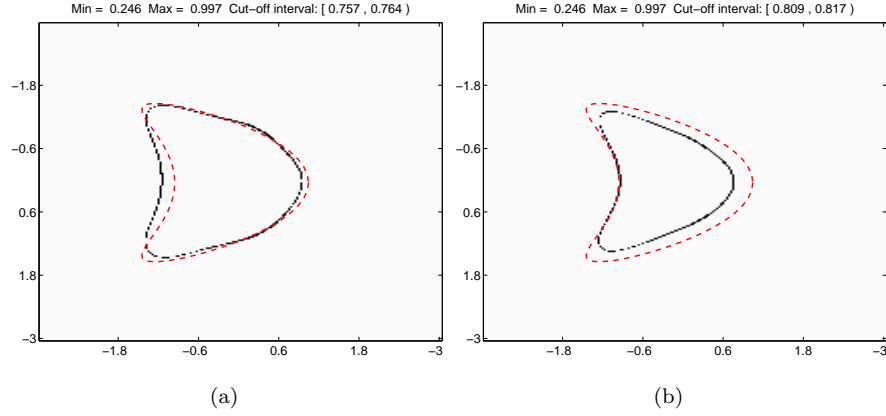


Figure 5: Level curves of  $\mathbb{I}^2(z)$  with  $N = 100$  (using the dipoles): (a)  $n = 69$ ; (b)  $n = 76$ . The dash curve represents the exact shape.

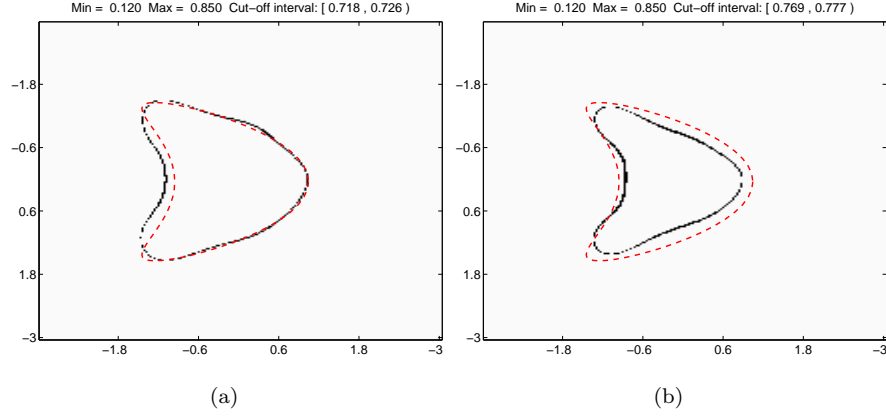


Figure 6: Level curves of  $\mathbb{I}^2(z)$  with  $N = 100$  (using the tripoles): (a)  $n = 83$ ; (b)  $n = 90$ . The dash curve represents the exact shape.

in Theorem 3.2, although the Theorem only deals with the limit (as the noise level tends to zero) of the indicator function.

We note that the level curves in the above examples depend on the heuristic parameter  $\frac{n}{N}$ . Although we cannot choose a fixed value which can guarantee good estimates for different shapes, the numerical results show that "the best" level curves for the considered obstacles in the case of monopole are obtained as  $n$  is around 90 for  $N = 100$ . That means,  $\frac{n}{N}$  is around 90%.

In analyzing the numerical results, we observed that the indicator function  $\mathbb{I}^2$  provides good estimates of the shape for all monopole, dipoles and tripoles, but it is not the case for  $\mathbb{I}^1$  when the dipoles and tripoles are used (see Figure 9). Hence, we should only use  $\mathbb{I}^2$  (or equivalently, the Herglotz wavefunction) as the indicator function for the dipoles and tripoles.

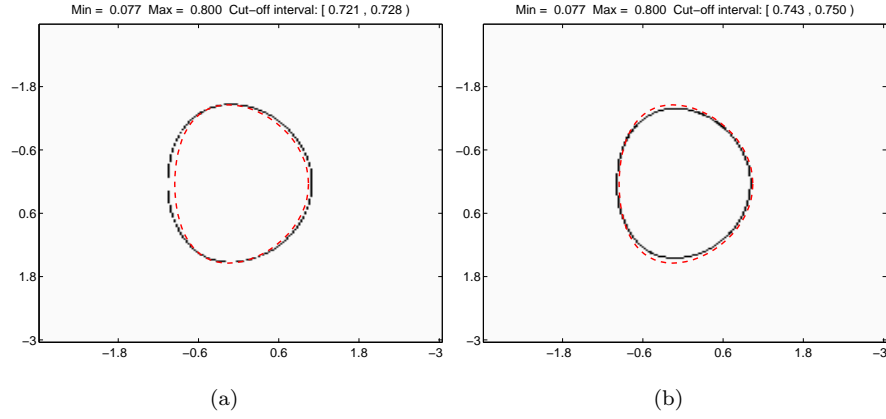


Figure 7: Level curves of  $\mathbb{I}^2(z)$  for the kite with  $c = 0.1$  and  $N = 100$  (using the monopole): (a)  $n = 90$ ; (b)  $n = 93$ . The dash curve represents the exact shape.

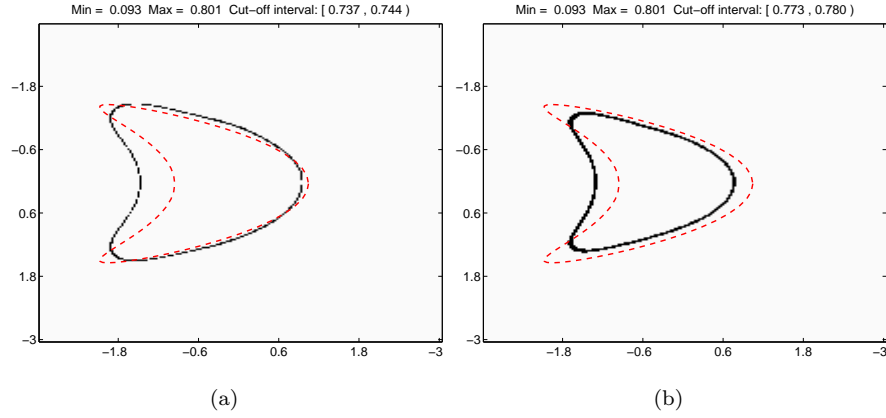


Figure 8: Level curves of  $\mathbb{I}^2(z)$  for the kite with  $c = 1$  and  $N = 100$  (using the monopole): (a)  $n = 92$ ; (b)  $n = 97$ . The dash curve represents the exact shape.

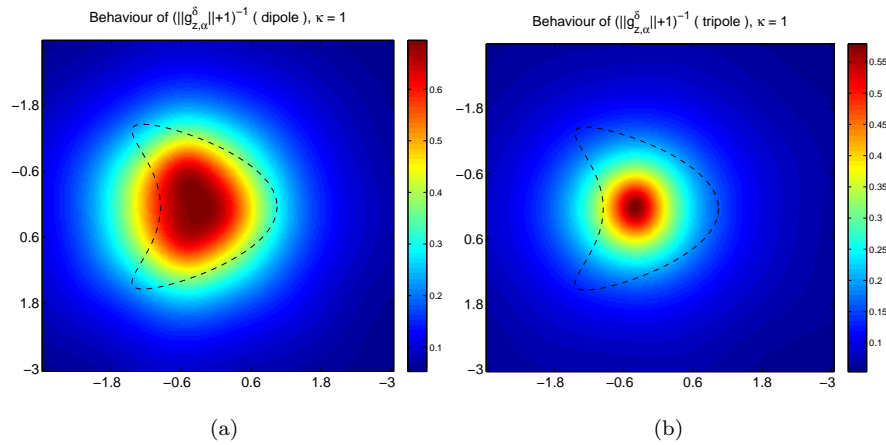


Figure 9: The behavior of the indicator function  $\mathbb{I}^1(z) = (\|g_{z,\alpha}^\delta\| + 1)^{-1}$ : (a) dipoles; (b) tripoles. The dash curve represents the exact shape.

### Comparison of the monopole, dipoles and tripoles:

Figures 4–6 show that the accuracy for the monopole, dipoles and tripoles are different on some portions of the obstacle’s boundary, especially on the concave part. To have a better comparison of the accuracy for the multipoles of different orders, we depict in Figures 10–12 the results for the three considered obstacles. In these figures, the reconstructed shapes of the obstacles are chosen as the ”best” level curves.

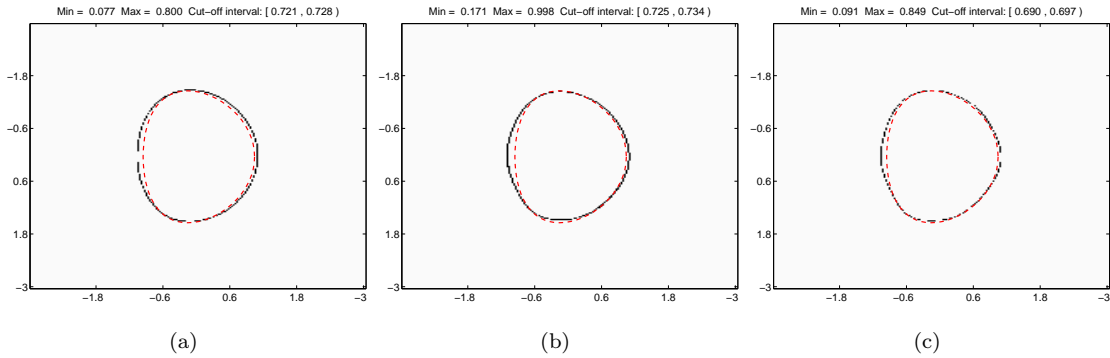


Figure 10: Reconstruction of the kite with  $c = 0.1$ : (a) monopole; (b) dipoles; (c) tripoles.

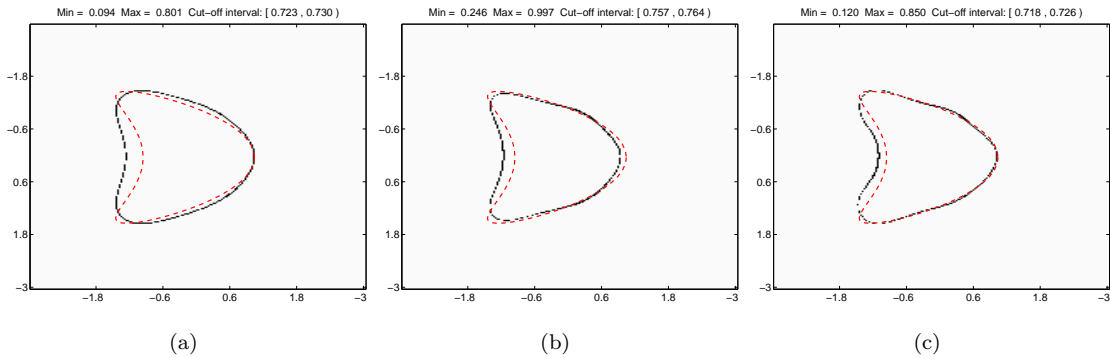


Figure 11: Reconstruction of the kite with  $c = 0.1$ : (a) monopole; (b) dipoles; (c) tripoles.

Figure 10 shows that if the curvature of the obstacle is rather uniform, the reconstruction accuracy is similar in all cases. However, if the curvature is not uniform (Figures 11 and 12), the accuracy is better for multipoles of higher order (especially in the concave part). Therefore, it is recommended to use multipoles instead of the monopole in the linear sampling method.

## 5 Conclusions and perspectives

We have demonstrated theoretically as well as numerically that the blowup rate of (the limit of) the indicator function in the linear sampling method near the boundary of an obstacle depends on its geometry for the case of Dirichlet boundary condition. This partly explains the accuracy of the linear sampling method. Moreover, in the case of impedance boundary condition, the impedance of the boundary of

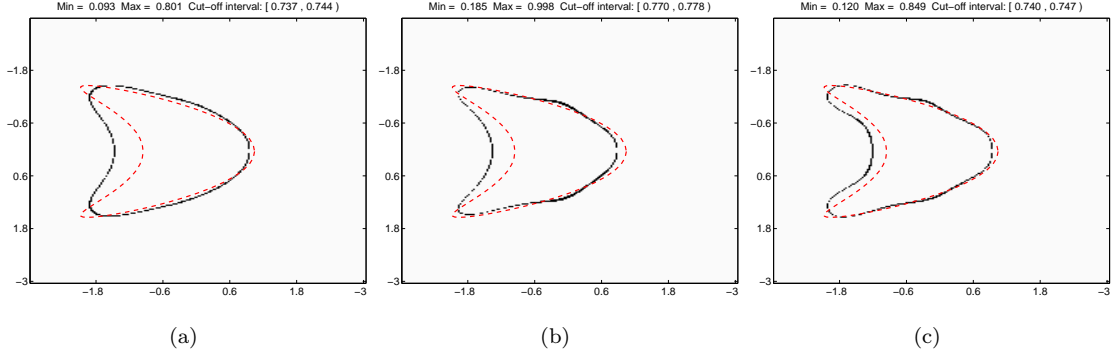


Figure 12: Reconstruction of the kite with  $c = 1$ : (a) monopole; (b) dipoles; (c) tripoles.

the obstacle should also be involved in the blowup rate of the indicator function. Therefore, in design problems, we can expect to be able to make the obstacle appear more or less clearly by coating its boundary with a material which reduces or increases the effect of the curvature on the blowup rate of the indicator function. This problem is under investigation.

## 6 Appendix: Proofs of Lemmas 3.7 and 3.8

The proofs of these lemmas for the monopole and multipoles are similar. Moreover, the curvature of the obstacle appears in the singular terms only in the case of tripoles. This is also the most complicated case. Hence, we only present the proofs for this case.

To prove these lemmas, we have to use the asymptotic expansions of the function  $\omega^+(\xi, \eta)$  and the Green's function  $G(\xi, \eta)$  (see (42)). The former was given in the end of the proof of Theorem 3.2. The latter is given in the following lemma.

**Lemma 6.1.** *The first derivatives of the Green's function  $G(\xi, \eta)$  for  $\xi, \eta \in Q$  close enough to the origin can be written as follows*

$$\begin{aligned} G_{\xi_1} &:= \frac{\partial G}{\partial \xi_1} = -\frac{1}{2\pi} \left[ \frac{\xi_1 - \eta_1}{|\xi - \eta|^2} - \frac{\xi_1 - \eta_1}{|\xi - \eta^*|^2} \right] + \frac{O(\eta_1)}{|\xi - \eta|} + O(1), \quad |\xi - \eta| \rightarrow 0, \\ G_{\xi_2} &:= \frac{\partial G}{\partial \xi_2} = -\frac{1}{2\pi} \left[ \frac{\xi_2 - \eta_2}{|\xi - \eta|^2} - \frac{\xi_2 + \eta_2}{|\xi - \eta^*|^2} \right] + \frac{O(\eta_1)}{|\xi - \eta|} + O(1), \quad |\xi - \eta| \rightarrow 0. \end{aligned} \quad (55)$$

*Remark 6.2.* Upper estimates of  $G$  and  $\nabla G$  are given in [15, 16] and some asymptotic expansions are also discussed in [14]. However, the explicit form (55) are missed there. Therefore, we give below the proof of this lemma for the completeness of the paper.

*Proof.* It was proved, e.g., in [17], that if  $M$  is a constant positive definite matrix, the Green's function  $G(\xi, \eta)$  can be written as

$$G(\xi, \eta) = \Phi^+(\xi, \eta),$$

where  $\Phi^+(\xi, \eta) := \tilde{\Phi}(\xi, \eta) - \tilde{\Phi}(\xi, \eta^*)$  with  $\tilde{\Phi}(\xi, \eta)$  being the fundamental solution of the equation

$$\nabla \cdot [M \nabla \tilde{\Phi}(\xi, \eta)] + \kappa^2 \tilde{\Phi}(\xi, \eta) = -\delta(\xi - \eta), \quad \xi \in \mathbb{R}^2.$$

In this paper, since the matrix  $M$  depends on the variable  $\xi$ , we do not have the above equality. However, to derive the derivatives of the Green's function  $G(\xi, \eta)$ , we also compare it with  $\Phi^+(\eta, \xi)$  (the reason for exchanging the order of  $\xi$  and  $\eta$  will be clear in the following, see (58)). To do so, we first note that  $\Phi^+(z, \eta)$  satisfies the equation

$$\nabla \cdot [M\nabla\Phi^+(z, \xi)] + \kappa^2\Phi^+(z, \xi) = -\delta(z - \xi) + \delta(z - \xi^*), \quad z \in \mathbb{R}^2. \quad (56)$$

We recall that  $G(z, \eta)$  is the solution of the problem

$$\begin{cases} \nabla \cdot [M\nabla G(z, \eta)] + \kappa^2 G(z, \eta) = -\delta(z - \eta), & z \in \mathbb{R}_+^2, \\ G(z, \eta) = 0, & z \in \partial\mathbb{R}_+^2. \end{cases} \quad (57)$$

Multiplying both sides of (56) and (57) by  $G(z, \eta)$  and  $\Phi^+(z, \xi)$ , respectively, taking the difference, integrating over  $Q$  and using the same arguments as in analyzing  $\tilde{R}(\xi, \eta)$  in the proof of Theorem 3.2, we obtain, for  $\xi, \eta \in Q$ ,

$$G(\xi, \eta) - \Phi^+(\eta, \xi) = \int_S M\nabla G(z, \eta) \cdot \nu \Phi^+(z, \xi) ds(z) + \int_{S^c} [M\nabla G(z, \eta) \cdot \nu \Phi^+(z, \xi) - M\nabla \Phi^+(z, \xi) \cdot \nu G(z, \eta)] ds(z). \quad (58)$$

Since the functions  $G(z, \eta)$  and  $\Phi^+(z, \xi)$  are regular on the boundary  $S^c$ , the second term on the right hand side of (65) is bounded with its derivatives with respect to  $\xi$ . Hence,

$$\frac{\partial G}{\partial \xi_j}(\xi, \eta) - \frac{\partial \Phi^+}{\partial \xi_j}(\eta, \xi) = \int_S M\nabla G(z, \eta) \cdot \nu \frac{\partial \Phi^+}{\partial \xi_j}(z, \xi) ds(z) + O(1), \quad j = 1, 2. \quad (59)$$

We now investigate the expansion of  $\Phi^+(\eta, \xi)$ . By changing the variable  $\bar{z} = \Theta^{-1}(\xi) = (\xi_1, \xi_2 + f(\xi_1))^T$ ,  $\bar{x} = \Theta^{-1}(\eta)$  and denote by  $\bar{\Phi}(\bar{x}, \bar{z}) = \tilde{\Phi}(\eta, \xi)$ , we have

$$\Delta_{\bar{x}} \bar{\Phi}(\bar{x}, \bar{z}) + \kappa^2 \bar{\Phi}(\bar{x}, \bar{z}) = -\delta(\Theta(\bar{x}) - \Theta(\bar{z})).$$

But we note that since  $\Theta$  is bijective, we have  $\delta(\Theta(\bar{x}) - \Theta(\bar{z})) = \delta(\bar{x} - \bar{z})$ . This implies that  $\bar{\Phi}(\bar{x}, \bar{z}) = \Phi(\bar{x}, \bar{z})$ . Therefore,

$$\Phi^+(\eta, \xi) = \Phi(\Theta^{-1}(\eta), \Theta^{-1}(\xi)) - \Phi(\Theta^{-1}(\eta), \Theta^{-1}(\xi^*)).$$

Consequently,

$$\begin{aligned} \frac{\partial \Phi^+(\eta, \xi)}{\partial \xi_1} &= \frac{\partial \Phi(\Theta^{-1}(\eta), \Theta^{-1}(\xi))}{\partial \bar{z}_1} + \frac{\partial \Phi(\Theta^{-1}(\eta), \Theta^{-1}(\xi))}{\partial \bar{z}_2} f'_a(\xi_1) \\ &\quad - \frac{\partial \Phi(\Theta^{-1}(\eta), \Theta^{-1}(\xi^*))}{\partial \bar{z}_1} - \frac{\partial \Phi(\Theta^{-1}(\eta), \Theta^{-1}(\xi^*))}{\partial \bar{z}_2} f'_a(\xi_1). \end{aligned}$$

Using Lemma 3.6, we obtain

$$\begin{aligned} \frac{\partial \Phi^+(\eta, \xi)}{\partial \xi_1} &= -\frac{1}{2\pi} \left[ \frac{\xi_1 - \eta_1}{|\Theta^{-1}(\eta) - \Theta^{-1}(\xi)|^2} - \frac{\xi_1 - \eta_1}{|\Theta^{-1}(\eta) - \Theta^{-1}(\xi^*)|^2} \right] \\ &\quad - \frac{f'_a(\xi_1)}{2\pi} \left[ \frac{\xi_2 - \eta_2 + f_a(\xi_1) - f_a(\eta_1)}{|\Theta^{-1}(\eta) - \Theta^{-1}(\xi)|^2} - \frac{-\xi_2 - \eta_2 + f_a(\xi_1) - f_a(\eta_1)}{|\Theta^{-1}(\eta) - \Theta^{-1}(\xi^*)|^2} \right] + O(|\eta - \xi| \ln |\eta - \xi|). \end{aligned} \quad (60)$$

Similarly,

$$\begin{aligned} \frac{\partial \Phi^+(\eta, \xi)}{\partial \xi_2} &= -\frac{1}{2\pi} \left[ \frac{\xi_2 - \eta_2}{|\Theta^{-1}(\eta) - \Theta^{-1}(\xi)|^2} - \frac{\xi_2 + \eta_2}{|\Theta^{-1}(\eta) - \Theta^{-1}(\xi^*)|^2} \right] \\ &\quad - \frac{1}{2\pi} \left[ \frac{f_a(\xi_1) - f_a(\eta_1)}{|\Theta^{-1}(\eta) - \Theta^{-1}(\xi)|^2} + \frac{f_a(\xi_1) - f_a(\eta_1)}{|\Theta^{-1}(\eta) - \Theta^{-1}(\xi^*)|^2} \right] + O(|\eta - \xi| \ln |\eta - \xi|). \end{aligned} \quad (61)$$

On the other hand,

$$|\Theta^{-1}(\xi) - \Theta^{-1}(\eta)|^2 = |\xi - \eta|^2 + 2(\eta_2 - \xi_2)[f_a(\eta_1) - f_a(\xi_1)] + [f_a(\eta_1) - f_a(\xi_1)]^2.$$

Using the Taylor expansion, we have

$$f_a(\eta_1) - f_a(\xi_1) = f'_a(\xi_1)(\eta_1 - \xi_1) + \frac{1}{2}f''_a(\xi_1)(\eta_1 - \xi_1)^2 + O((\xi_1 - \eta_1)^3).$$

Here we have used the Lipschitz condition for the second derivative of  $f_a$ . Hence,

$$\begin{aligned} |\Theta^{-1}(\xi) - \Theta^{-1}(\eta)|^2 &= |\xi - \eta|^2 \left\{ 1 + 2f'_a(\xi_1) \frac{(\eta_1 - \xi_1)(\eta_2 - \xi_2)}{|\xi - \eta|^2} + f''_a(\xi_1) \frac{(\eta_2 - \xi_2)(\eta_1 - \xi_1)^2}{|\xi - \eta|^2} \right. \\ &\quad \left. + [f'_a(\xi_1)]^2 \frac{(\eta_1 - \xi_1)^2}{|\xi - \eta|^2} + f'_a(\xi_1)f''_a(\xi_1) \frac{(\eta_1 - \xi_1)^3}{|\xi - \eta|^2} + O((\xi_1 - \eta_1)^2) \right\}. \end{aligned}$$

We note that  $f'(\xi_1) = O(\xi_1)$ . Hence we can choose a fixed value  $\tilde{\xi}_1 > 0$  such that for  $|\xi_1| < \tilde{\xi}_1$  and  $\eta$  close enough to  $\xi$ , the absolute value of the sum of the last five terms on the right hand side is less than 1.

Using the equality

$$\frac{1}{1+x} = 1 - x + x^2 - \dots$$

for  $|x| < 1$ , we obtain

$$\begin{aligned} \frac{1}{|\Theta^{-1}(\xi) - \Theta^{-1}(\eta)|^2} &= \frac{1}{|\xi - \eta|^2} \left\{ 1 - 2f'_a(\xi_1) \frac{(\eta_1 - \xi_1)(\eta_2 - \xi_2)}{|\xi - \eta|^2} - f''_a(\xi_1) \frac{(\eta_2 - \xi_2)(\eta_1 - \xi_1)^2}{|\xi - \eta|^2} \right. \\ &\quad \left. + [f'_a(\xi_1)]^2 O(1) + f'_a(\xi_1)O(\eta_1 - \xi_1) + O((\xi_1 - \eta_1)^2) \right\}. \end{aligned} \quad (62)$$

Using the same arguments as above, with  $\xi$  being replaced by  $\xi^*$  and the note that  $|\eta - \xi^*| \geq |\eta - \xi|$  for  $\xi, \eta \in Q$ , we obtain

$$\begin{aligned} \frac{1}{|\Theta^{-1}(\xi^*) - \Theta^{-1}(\eta)|^2} &= \frac{1}{|\xi^* - \eta|^2} \left\{ 1 - 2f'_a(\xi_1) \frac{(\eta_1 - \xi_1)(\eta_2 + \xi_2)}{|\xi^* - \eta|^2} - f''_a(\xi_1) \frac{(\eta_2 + \xi_2)(\eta_1 - \xi_1)^2}{|\xi^* - \eta|^2} \right. \\ &\quad \left. + [f'_a(\xi_1)]^2 O(1) + f'_a(\xi_1)O(\eta_1 - \xi_1) + O((\xi_1 - \eta_1)^2) \right\}. \end{aligned} \quad (63)$$

Note that  $f'_a(\xi_1) = f'_a(\eta_1) + O(\xi_1 - \eta_1)$ . Moreover,  $f'_a(\eta_1) = O(\eta_1)$ . Therefore, it follows from (60)–(63) that

$$\begin{aligned} \frac{\partial \Phi^+(\eta, \xi)}{\partial \xi_1} &= -\frac{1}{2\pi} \left[ \frac{\xi_1 - \eta_1}{|\xi - \eta|^2} - \frac{\xi_1 - \eta_1}{|\xi^* - \eta|^2} \right] + \frac{O(\eta_1)}{|\xi - \eta|} + O(1) \\ \frac{\partial \Phi^+(\eta, \xi)}{\partial \xi_2} &= -\frac{1}{2\pi} \left[ \frac{\xi_2 - \eta_2}{|\xi - \eta|^2} - \frac{\xi_2 + \eta_2}{|\xi^* - \eta|^2} \right] + \frac{O(\eta_1)}{|\xi - \eta|} + O(1). \end{aligned} \quad (64)$$

In particular, replacing  $\eta$  by  $z$  with  $z_2 = 0$ , we have

$$\frac{\partial \Phi^+(z, \xi)}{\partial \xi_1} = -\frac{1}{2\pi} \left\{ f'_a(\xi_1) \frac{O(1)}{|\xi - z|} + \xi_2 \frac{O(1)}{|\xi - z|} + O(\xi - z) \right\}.$$

A similar estimate also holds for  $\frac{\partial \Phi^+(z, \xi)}{\partial \xi_2}$ . On the other hand, the Green's function can be estimated as  $|\nabla G(z, \xi)| \leq C|z - \xi|^{-1}$  (see, e.g. [15, 16]). From these estimates we can prove that the integral on the right hand side of (59) is bounded. Finally, we note that  $|\xi^* - \eta| = |\xi - \eta^*|$ . This completes the proof.  $\square$

### Proof of Lemma 3.7

We have from (39) that

$$\begin{aligned} (I - M)\nabla\omega^+ \cdot \nabla G &= f'_a(\xi_1) \left[ \omega_{\xi_2}^+ G_{\xi_1} + \omega_{\xi_1}^+ G_{\xi_2} \right] - (f'_a(\xi_1))^2 \omega_{\xi_2}^+ G_{\xi_2} \\ &= f'_a(\eta_1) \left[ \omega_{\xi_2}^+ G_{\xi_1} + \omega_{\xi_1}^+ G_{\xi_2} \right] - (f'_a(\xi_1))^2 \omega_{\xi_2}^+ G_{\xi_2} \\ &\quad + [f'_a(\xi_1) - f'_a(\eta_1)] \left[ \omega_{\xi_2}^+ G_{\xi_1} + \omega_{\xi_1}^+ G_{\xi_2} \right] \end{aligned}$$

On the other hand, under the hypothesis  $f \in C^{2,1}[-r, r]$  we obtain the expansion of  $f'_a(\xi_1)$  at  $\xi_1 = \eta_1$  as

$$f'_a(\xi_1) = f'_a(\eta_1) + f''_a(\eta_1)(\xi_1 - \eta_1) + O((\xi_1 - \eta_1)^2). \quad (65)$$

Moreover,

$$f'_a(\eta_1) = f''_a(0)\eta_1 + O(\eta_1^2). \quad (66)$$

Substituting these equalities into (44), we have

$$\begin{aligned} I_1 &= \int_Q (I - M)\nabla\omega^+(\xi, \eta) \cdot \nabla G(\xi, \eta) d\xi \\ &= f'_a(\eta_1) \int_Q \left[ \omega_{\xi_2}^+ G_{\xi_1} + \omega_{\xi_1}^+ G_{\xi_2} \right] (\xi, \eta) d\xi + f''_a(\eta_1) \int_Q (\xi_1 - \eta_1) \left[ \omega_{\xi_2}^+ G_{\xi_1} + \omega_{\xi_1}^+ G_{\xi_2} \right] (\xi, \eta) d\xi \\ &\quad + \int_Q O((\xi_1 - \eta_1)^2) \left[ \omega_{\xi_2}^+ G_{\xi_1} + \omega_{\xi_1}^+ G_{\xi_2} \right] (\xi, \eta) d\xi - \int_Q (f'_a(\xi_1))^2 \omega_{\xi_2}^+ (\xi, \eta) G_{\xi_2} (\xi, \eta) d\xi \\ &= I_1^1 + I_1^2 + I_1^3, \end{aligned}$$

where

$$I_1^1 = f'_a(\eta_1) \int_Q \left[ \omega_{\xi_2}^+ G_{\xi_1} + \omega_{\xi_1}^+ G_{\xi_2} \right] (\xi, \eta) d\xi, \quad (67)$$

$$I_1^2 = f''_a(\eta_1) \int_Q (\xi_1 - \eta_1) \left[ \omega_{\xi_2}^+ G_{\xi_1} + \omega_{\xi_1}^+ G_{\xi_2} \right] (\xi, \eta) d\xi, \quad (68)$$

$$I_1^3 = \int_Q O((\xi_1 - \eta_1)^2) \left[ \omega_{\xi_2}^+ G_{\xi_1} + \omega_{\xi_1}^+ G_{\xi_2} \right] (\xi, \eta) d\xi - \int_Q (f'_a(\xi_1))^2 \omega_{\xi_2}^+ (\xi, \eta) G_{\xi_2} (\xi, \eta) d\xi. \quad (69)$$

In the following, we show the detail proof for Case 3.1. The analysis is similar for Case 3.2. In this case, we have

$$\omega^+(\xi, \eta) = -\frac{\partial^2}{\partial \eta_1^2} \Phi(\xi, \eta^*) = -\frac{(\xi_1 - \eta_1)^2 - (\xi_2 + \eta_2)^2}{2\pi|\xi - \eta^*|^4} + O(\ln|\xi - \eta^*|).$$

By the same method for obtaining the equalities of Lemma 3.6, we can calculate the derivatives of  $\omega^+$  as

$$\begin{aligned}\omega_{\xi_1}^+(\xi, \eta) &= \frac{1}{\pi} \frac{(\xi_1 - \eta_1)[(\xi_1 - \eta_1)^2 - 3(\xi_2 + \eta_2)^2]}{|\xi - \eta^*|^6} + O(|\xi - \eta^*|^{-1}), \\ \omega_{\xi_2}^+(\xi, \eta) &= \frac{1}{\pi} \frac{(\xi_2 + \eta_2)[3(\xi_1 - \eta_1)^2 - (\xi_2 + \eta_2)^2]}{|\xi - \eta^*|^6} + O(|\xi - \eta^*|^{-1}).\end{aligned}$$

Hence

$$\begin{aligned}\omega_{\xi_2}^+ G_{\xi_1} + \omega_{\xi_1}^+ G_{\xi_2} &= -\frac{1}{2\pi^2} \left\{ \frac{(\xi_2 + \eta_2)[3(\xi_1 - \eta_1)^2 - (\xi_2 + \eta_2)^2]}{|\xi - \eta^*|^6} \left[ \frac{\xi_1 - \eta_1}{|\xi - \eta|^2} - \frac{\xi_1 - \eta_1}{|\xi - \eta^*|^2} \right] \right. \\ &\quad \left. + \frac{(\xi_1 - \eta_1)[(\xi_1 - \eta_1)^2 - 3(\xi_2 + \eta_2)^2]}{|\xi - \eta^*|^6} \left[ \frac{\xi_2 - \eta_2}{|\xi - \eta|^2} - \frac{\xi_2 + \eta_2}{|\xi - \eta^*|^2} \right] \right\} + J(\xi, \eta, \eta^*), \\ &= -\frac{\bar{\xi}_1}{2\pi^2} \left\{ \frac{\bar{\xi}_2(3\bar{\xi}_1^2 - \bar{\xi}_2^2) + (\bar{\xi}_2 - 2\eta_2)(\bar{\xi}_1^2 - 3\bar{\xi}_2^2)}{(\bar{\xi}_1^2 + \bar{\xi}_2^2)^3[\bar{\xi}_1^2 + (\bar{\xi}_2 - 2\eta_2)^2]} - \frac{4\bar{\xi}_2(\bar{\xi}_1^2 - \bar{\xi}_2^2)}{(\bar{\xi}_1^2 + \bar{\xi}_2^2)^4} \right\} + J(\xi, \eta, \eta^*).\end{aligned}$$

Here the function  $J(\xi, \eta, \eta^*)$  can be evaluated as

$$|J(\xi, \eta, \eta^*)| \leq O(|\xi - \eta^*|^{-1}) \left[ \frac{1}{|\xi - \eta|} + \frac{1}{|\xi - \eta^*|} \right] + \frac{O(\eta_1)}{|\xi - \eta||\xi - \eta^*|^3} + \frac{O(1)}{|\xi - \eta^*|^3}.$$

Since for all  $\xi \in Q$  we have  $|\xi - \eta^*| \geq \eta_2$ , thus

$$\begin{aligned}\int_Q O(|\xi - \eta^*|^{-1}) \left[ \frac{1}{|\xi - \eta|} + \frac{1}{|\xi - \eta^*|} \right] d\xi &\leq C(\ln \eta_2 + 1), \\ \int_Q \frac{O(\eta_1)}{|\xi - \eta||\xi - \eta^*|^3} d\xi &\leq \frac{1}{\eta_2^{2-\epsilon}} \int_Q \frac{O(\eta_1)}{|\xi - \eta||\xi - \eta^*|^{1+\epsilon}} d\xi \leq \frac{O(\eta_1)}{\eta_2^{2-\epsilon}\eta_2^\epsilon} = \frac{O(\eta_1)}{\eta_2^2}, \\ \int_Q \frac{O(1)}{|\xi - \eta^*|^3} d\xi &\leq \frac{O(1)}{\eta_2},\end{aligned}$$

for  $0 < \epsilon < 1$  (see also [18], Lemmas 4.1 and 4.4). From these inequalities we have

$$f'(\eta_1) \int_Q J(\xi, \eta, \eta^*) d\xi = O(1).$$

Using similar arguments, we can prove that

$$\int_Q (\xi_1 - \eta_1) J(\xi, \eta, \eta^*) d\xi = O(\ln \eta_2).$$

We note that the highest singular terms of  $I_1^1$  are odd functions of  $\bar{\xi}_1$ , therefore  $I_1^1 = O(1)$ .

We write the term  $I_1^2$  as follows

$$I_1^2 = -\frac{f_a''(\eta_1)}{2\pi^2} (T_1 + T_2) + O(\ln \eta_2),$$

where

$$\begin{aligned}T_1 &= \int_{\eta_2}^{r_2+\eta_2} d\bar{\xi}_2 \int_{-r_1}^{r_1} \bar{\xi}_1^2 \frac{\bar{\xi}_2(3\bar{\xi}_1^2 - \bar{\xi}_2^2) + (\bar{\xi}_2 - 2\eta_2)(\bar{\xi}_1^2 - 3\bar{\xi}_2^2)}{(\bar{\xi}_1^2 + \bar{\xi}_2^2)^3[\bar{\xi}_1^2 + (\bar{\xi}_2 - 2\eta_2)^2]} d\bar{\xi}_1, \\ T_2 &= - \int_{\eta_2}^{r_2+\eta_2} d\bar{\xi}_2 \int_{-r_1}^{r_1} \bar{\xi}_1^2 \frac{4\bar{\xi}_2(\bar{\xi}_1^2 - \bar{\xi}_2^2)}{(\bar{\xi}_1^2 + \bar{\xi}_2^2)^4} d\bar{\xi}_1.\end{aligned}$$

By direct and elementary manipulations we obtain

$$-\int_{-r_1}^{r_1} \bar{\xi}_1^2 \frac{4\bar{\xi}_2(\bar{\xi}_1^2 - \bar{\xi}_2^2)}{(\bar{\xi}_1^2 + \bar{\xi}_2^2)^4} d\bar{\xi}_1 = \frac{8}{3} \frac{\bar{\xi}_2 r_1}{(r_1^2 + \bar{\xi}_2^2)^2} - \frac{8}{3} \frac{\bar{\xi}_2^2 r_1}{(r_1^2 + \bar{\xi}_2^2)^3}.$$

Using the fact that  $r_1^2 + \bar{\xi}_2^2 \geq r_1^2$  we see that the integration with respect to  $\bar{\xi}_2$  is bounded. Hence,  $T_2$  is bounded. The term  $T_1$  can also be proved to be bounded with a bit more complicated (but elementary) manipulations. In deed, integrating over  $\bar{\xi}_1$ , we have

$$T_1 = \int_{\eta_2}^{r_2 + \eta_2} \left\{ \frac{(\bar{\xi}_2 - 2\eta_2)}{4\eta_2^3} \left[ \arctan\left(\frac{r_1}{\bar{\xi}_2 - 2\eta_2}\right) - \arctan\left(\frac{r_1}{\bar{\xi}_2}\right) \right] + \frac{r_1^3}{\eta_2(r_1^2 + \bar{\xi}_2^2)^2} - \frac{r_1 \bar{\xi}_2}{2\eta_2^2(r_1^2 + \bar{\xi}_2^2)} \right\} d\bar{\xi}_2.$$

Now we consider  $g(\eta_2) = \arctan\left(\frac{r_1}{\bar{\xi}_2 - 2\eta_2}\right)$  as a function of  $\eta_2$ . By explicit calculations we can see that it has bounded derivatives up to the third order. Thus, around  $\eta_2 = 0$  it can be represented by the Taylor series as

$$g(\eta_2) = \arctan\left(\frac{r_1}{\bar{\xi}_2}\right) + \frac{2r_1}{r_1^2 + \bar{\xi}_2^2} \eta_2 + \frac{4\bar{\xi}_2 r_1}{(r_1^2 + \bar{\xi}_2^2)^2} \eta_2^2 + O(1)\eta_2^3.$$

Substituting this into the above equation, we have

$$\begin{aligned} T_1 &= \int_{\eta_2}^{r_2 + \eta_2} \left\{ \frac{(\bar{\xi}_2 - 2\eta_2)}{4\eta_2^3} \left[ \frac{2r_1}{r_1^2 + \bar{\xi}_2^2} \eta_2 + \frac{4\bar{\xi}_2 r_1}{(r_1^2 + \bar{\xi}_2^2)^2} \eta_2^2 \right] + \frac{r_1^3}{\eta_2(r_1^2 + \bar{\xi}_2^2)^2} - \frac{r_1 \bar{\xi}_2}{2\eta_2^2(r_1^2 + \bar{\xi}_2^2)} \right\} d\bar{\xi}_2 + O(1) \\ &= \int_{\eta_2}^{r_2 + \eta_2} \left\{ \frac{(\bar{\xi}_2 - 2\eta_2)r_1}{2\eta_2^2(r_1^2 + \bar{\xi}_2^2)} - \frac{r_1 \bar{\xi}_2}{2\eta_2^2(r_1^2 + \bar{\xi}_2^2)} + \frac{r_1 \bar{\xi}_2 (\bar{\xi}_2 - 2\eta_2)}{\eta_2 (r_1^2 + \bar{\xi}_2^2)^2} + \frac{r_1^3}{\eta_2 (r_1^2 + \bar{\xi}_2^2)^2} \right\} d\bar{\xi}_2 + O(1) \\ &= - \int_{\eta_2}^{r_2 + \eta_2} \frac{2r_1 \bar{\xi}_2}{(r_1^2 + \bar{\xi}_2^2)^2} d\bar{\xi}_2 + O(1) = O(1). \end{aligned}$$

From the above analysis, we have  $I_1^2 = O(\ln \eta_2)$ . Since  $I_1^3$  is more regular than the other two terms, we conclude that  $I_1 = O(\ln \eta_2)$ .  $\square$

### Proof of Lemma 3.8

We note that the unit normal vector of  $S$  is  $\nu = (0, -1)$ . It follows from (44) that

$$M\nabla G \cdot \nu|_S = -\frac{\partial G}{\partial \xi_2} + f'_a(\xi_1) \frac{\partial G}{\partial \xi_1} - (f'_a(\xi_1))^2 \frac{\partial G}{\partial \xi_2}.$$

Substituting this into (44) we obtain

$$I_2 = I_2^1 + I_2^2,$$

where

$$\begin{aligned} I_2^1 &= - \int_S \frac{\partial G}{\partial \xi_2}(\xi, \eta) \tilde{R}(\xi, \eta) d\xi_1, \\ I_2^2 &= \int_S f'_a(\xi_1) \frac{\partial G}{\partial \xi_1}(\xi, \eta) \tilde{R}(\xi, \eta) d\xi_1 - \int_S (f'_a(\xi_1))^2 \frac{\partial G}{\partial \xi_2}(\xi, \eta) \tilde{R}(\xi, \eta) d\xi_1. \end{aligned} \tag{70}$$

It is clear that  $I_2^1$  is more singular than  $I_2^2$ , so in the following, we only evaluate this term to find the highest singular behavior of  $I_2$ . Since for  $\xi \in S$  we have  $\xi_2 = 0$ , therefore  $|\xi - \eta| = |\xi - \eta^*|$ . It follows from (55) that

$$\frac{\partial G}{\partial \xi_2}(\xi, \eta)|_S = \frac{1}{\pi} \frac{\eta_2}{|\xi - \eta|^2} + \frac{O(\eta_1)}{|\xi - \eta|} + O(1).$$

Replacing this into (70) and using the boundary condition of (41) we arrive at

$$\begin{aligned} I_2^1 &= \frac{\eta_2}{\pi} \int_{-r_1+\eta_1}^{r_1+\eta_1} \frac{\bar{\psi}(\Theta^{-1}(\xi), \Theta^{-1}(\eta)) - \bar{\psi}(\xi, \eta)}{|\xi - \eta|^2} d\xi_1 \\ &+ \int_{-r_1+\eta_1}^{r_1+\eta_1} \left[ \frac{O(\eta_1)}{|\xi - \eta|} + O(1) \right] [\bar{\psi}(\Theta^{-1}(\xi), \Theta^{-1}(\eta)) - \bar{\psi}(\xi, \eta)] d\xi_1. \end{aligned} \quad (71)$$

Let us consider the following cases.

**Case 3.1:**  $\bar{\psi}(\bar{x}, \bar{z}) = \frac{\partial^2}{\partial \bar{z}^2} \Phi(\bar{x}, \bar{z})$ . In this case, we have

$$\bar{\psi}(\bar{x}, \bar{z}) = \frac{1}{2\pi} \frac{(\bar{x}_1 - \bar{z}_1)^2 - (\bar{x}_2 - \bar{z}_2)^2}{|\bar{x} - \bar{z}|^4} + O(\ln |\xi - \eta|),$$

hence

$$\begin{aligned} &\bar{\psi}(\Theta^{-1}(\xi), \Theta^{-1}(\eta)) - \bar{\psi}(\xi, \eta) \\ &= \frac{1}{2\pi} \left\{ \frac{(\xi_1 - \eta_1)^2 - [-\eta_2 + f_a(\xi_1) - f_a(\eta_1)]^2}{|\Theta^{-1}(\xi) - \Theta^{-1}(\eta)|^4} - \frac{(\xi_1 - \eta_1)^2 - \eta_2^2}{|\xi - \eta|^4} \right\} + O(\ln |\xi - \eta|). \end{aligned}$$

Since this function is more singular, we need more terms in the Taylor expansion of  $|\Theta^{-1}(\xi) - \Theta^{-1}(\eta)|^{-4}$  than in (62). Using the same arguments in deriving (62), we have

$$\frac{1}{|\Theta^{-1}(\xi) - \Theta^{-1}(\eta)|^4} = \frac{1 + 4\eta_2 f'_a(\eta_1) \frac{\xi_1 - \eta_1}{|\xi - \eta|^2} + 2\eta_2 f''_a(\eta_1) \frac{(\xi_1 - \eta_1)^2}{|\xi - \eta|^2} + O(|\xi - \eta|^2)}{|\xi - \eta|^4}. \quad (72)$$

Therefore,

$$\begin{aligned} &\frac{(\xi_1 - \eta_1)^2 - [-\eta_2 + f_a(\xi_1) - f_a(\eta_1)]^2}{|\Theta^{-1}(\xi) - \Theta^{-1}(\eta)|^4} \\ &= \frac{(\xi_1 - \eta_1)^2 - \eta_2^2 + 2\eta_2 [f'_a(\eta_1)(\xi_1 - \eta_1) + \frac{1}{2} f''_a(\eta_1)(\xi_1 - \eta_1)^2 + O(|\xi - \eta|^3)]}{|\xi - \eta|^4} \\ &\times \left[ 1 + 4\eta_2 f'_a(\eta_1) \frac{\xi_1 - \eta_1}{|\xi - \eta|^2} + 2\eta_2 f''_a(\eta_1) \frac{(\xi_1 - \eta_1)^2}{|\xi - \eta|^2} + O(|\xi - \eta|^2) \right] \\ &= \frac{1}{|\xi - \eta|^4} \left\{ (\xi_1 - \eta_1)^2 - \eta_2^2 + 2\eta_2 f'_a(\eta_1)(\xi_1 - \eta_1) + \eta_2 f''_a(\eta_1)(\xi_1 - \eta_1)^2 \right. \\ &\left. + [(\xi_1 - \eta_1)^2 - \eta_2^2] 4\eta_2 f'_a(\eta_1) \frac{\xi_1 - \eta_1}{|\xi - \eta|^2} + [(\xi_1 - \eta_1)^2 - \eta_2^2] 2\eta_2 f''_a(\eta_1) \frac{(\xi_1 - \eta_1)^2}{|\xi - \eta|^2} \right\} + O(1). \end{aligned}$$

Consequently,

$$\begin{aligned} \bar{\psi}(\Theta^{-1}(\xi), \Theta^{-1}(\eta)) - \bar{\psi}(\xi, \eta) &= \frac{1}{2\pi |\xi - \eta|^4} \left\{ 2\eta_2 f'_a(\eta_1)(\xi_1 - \eta_1) + \eta_2 f''_a(\eta_1)(\xi_1 - \eta_1)^2 \right. \\ &\left. + [(\xi_1 - \eta_1)^2 - \eta_2^2] 4\eta_2 f'_a(\eta_1) \frac{\xi_1 - \eta_1}{|\xi - \eta|^2} + [(\xi_1 - \eta_1)^2 - \eta_2^2] 2\eta_2 f''_a(\eta_1) \frac{(\xi_1 - \eta_1)^2}{|\xi - \eta|^2} \right\} + O(\ln |\xi - \eta|). \end{aligned}$$

We see that the first and the third terms are odd with respect to  $\xi_1 - \eta_1$ , so their integrals over  $S$  are eliminated. Moreover,  $|\ln |\xi - \eta|| \leq |\ln \eta_2|$  for  $|\xi - \eta| < 1$ . Hence, using elementary manipulations, we have

$$\begin{aligned} I_2^1 &= \frac{\eta_2^2 f_a''(\eta_1)}{2\pi^2} \int_{-r_1+\eta_1}^{r_1+\eta_1} \frac{(\xi_1 - \eta_1)^2 |\xi - \eta|^2 + 2(\xi_1 - \eta_1)^2 [(\xi_1 - \eta_1)^2 - \eta_2^2]}{|\xi - \eta|^8} d\xi_1 + O(\ln \eta_2) \\ &= \frac{\eta_2^2 f_a''(\eta_1)}{2\pi^2} \int_{-r_1}^{r_1} \frac{\bar{\xi}_1^2 [3\bar{\xi}_1^2 - \eta_2^2]}{(\bar{\xi}_1^2 + \eta_2^2)^4} d\bar{\xi}_1 + O(\ln \eta_2) \\ &= \frac{\eta_2^2 f_a''(\eta_1)}{2\pi^2} \frac{\pi}{8\eta_2^3} + O(\ln \eta_2) = \frac{f_a''(0)}{16\pi\eta_2} + O(\ln \eta_2). \end{aligned}$$

Here we have used the Lipschitz condition of  $f_a''$ , i.e.  $|f_a''(\eta_1) - f_a''(0)| \leq |\eta_1| \leq \eta_2 \tan \theta$ .

**Case 3.2:**  $\bar{\psi}(\bar{x}, \bar{z}) = \frac{\partial^2}{\partial \bar{z}_1 \partial \bar{z}_2} \Phi(\bar{x}, \bar{z})$ . Similar to the previous case, we have

$$\bar{\psi}(\bar{x}, \bar{z}) = \frac{1}{\pi} \frac{(\bar{x}_1 - \bar{z}_1)(\bar{x}_2 - \bar{z}_2)}{|\bar{x} - \bar{z}|^4} + O(\ln |\xi - \eta|),$$

and hence using (72) again, we obtain

$$\begin{aligned} \bar{\psi}(\Theta^{-1}(\xi), \Theta^{-1}(\eta)) - \bar{\psi}(\xi, \eta) &= \frac{1}{\pi |\xi - \eta|^4} \left\{ -4\eta_2^2 f_a'(\eta_1) \frac{(\xi_1 - \eta_1)^2}{|\xi - \eta|^2} - 2\eta_2^2 f_a''(\eta_1) \frac{(\xi_1 - \eta_1)^3}{|\xi - \eta|^2} \right. \\ &\quad \left. + f_a'(\eta_1)(\xi_1 - \eta_1)^2 + \frac{1}{2} f_a''(\eta_1)(\xi_1 - \eta_1)^3 \right\} + O(\ln \eta_2). \end{aligned}$$

We can see that the second and the fourth terms are odd functions of  $\xi_1 - \eta_1$ , so their integrals over  $S$  are eliminated. Hence,

$$\begin{aligned} I_2^1 &= \frac{\eta_2 f_a'(\eta_1)}{\pi^2} \int_{-r_1+\eta_1}^{r_1+\eta_1} \frac{(\xi_1 - \eta_1)^2 |\xi - \eta|^2 - 4\eta_2^2 (\xi_1 - \eta_1)^2}{|\xi - \eta|^8} d\xi_1 + O(\ln \eta_2) \\ &= \frac{\eta_2 f_a'(\eta_1)}{\pi^2} \int_{-r_1}^{r_1} \frac{\bar{\xi}_1^2 [\bar{\xi}_1^2 - 3\eta_2^2]}{(\bar{\xi}_1^2 + \eta_2^2)^4} d\bar{\xi}_1 + O(\ln \eta_2) \\ &= -\frac{f_a''(0)\eta_1}{8\pi\eta_2^2} + O(\ln \eta_2). \end{aligned}$$

The proof is complete. □

## Acknowledgements

This work was supported by the Johann Radon Institute for Computational and Applied Mathematics (RICAM), Austrian Academy of Sciences. The authors thank the referees for their useful comments and suggestions for improving this paper.

## References

- [1] T. Arens. Why linear sampling works. *Inverse Problems*, 20(1):163–173, 2004.

- [2] T. Arens and A. Lechleiter. The linear sampling method revisited. *Integral Equations and Applications*, 21(2):179–202, 2009.
- [3] M. Brignone, G. Bozza, R. Aramini, M. Pastorino, and M. Piana. A fully no-sampling formulation of the linear sampling method for three-dimensional inverse electromagnetic scattering problems. *Inverse Problems*, 25(1):015014, 20pp, 2009.
- [4] F. Cakoni and D. Colton. *Qualitative Methods in Inverse Scattering Theory*. Springer, 2006.
- [5] D. Colton and A. Kirsch. A simple method for solving inverse scattering problems in the resonance region. *Inverse Problems*, 12(4):383–393, 1996.
- [6] D. Colton and R. Kress. *Inverse acoustic and electromagnetic scattering theory*, volume 93 of *Applied Mathematical Sciences*. Springer-Verlag, Berlin, second edition, 1998.
- [7] P. Hähner. An inverse problem in electrostatics. *Inverse Problems*, 15(4):961–975, 1999.
- [8] M. Hanke. Why linear sampling really seems to work. *Inverse Probl. Imaging*, 2(3):373–395, 2008.
- [9] V. Isakov. *Inverse Problems for Partial Differential Equations*, volume 127 of *Applied Mathematical Sciences*. Springer Science+Business Media, Inc., New York, second edition, 2006.
- [10] A. Kirsch and N. Grinberg. *The factorization method for inverse problems*, volume 36 of *Oxford Lecture Series in Mathematics and its Applications*. Oxford University Press, Oxford, 2008.
- [11] J. Liu and M. Sini. On the accuracy of the numerical detection of complex obstacles from far field data using the probe method. *SIAM J. Sci. Comput.*, 31(4):2665–2687, 2009.
- [12] J. J. Liu, G. Nakamura, and M. Sini. Reconstruction of the shape and surface impedance from acoustic scattering data for an arbitrary cylinder. *SIAM J. Appl. Math.*, 67(4):1124–1146 (electronic), 2007.
- [13] W. McLean. *Strongly elliptic systems and boundary integral equations*. Cambridge University Press, Cambridge, 2000.
- [14] C. Miranda. *Partial differential equations of elliptic type*. Springer-Verlag, New York, 1970. Second revised edition. Translated from the Italian by Zane C. Motteler.
- [15] V. A. Solonnikov. The Green’s matrices for elliptic boundary value problems. I. *Trudy Mat. Inst. Steklov.*, 110:107–145, 1970.
- [16] V. A. Solonnikov. The Green’s matrices for elliptic boundary value problems. II. *Trudy Mat. Inst. Steklov.*, 116:181–216, 237, 1971. Boundary value problems of mathematical physics, 7.
- [17] R. C. Stevenson. Green’s function for the Helmholtz equation of a scalar wave in an anisotropic halfspace. *SIAM J. Appl. Math.*, 50(1):199–215, 1990.

- [18] N. Valdivia. Uniqueness in inverse obstacle scattering with conductive boundary conditions. *Appl. Anal.*, 83(8):825–851, 2004.